2-1-2011

Measurement, modeling and perception of painted surfaces : A Multi-scale analysis of the touch-up problem

Suparna Kalghatgi

Rochester Institute of Technology

MEASUREMENT, MODELING AND PERCEPTION OF PAINTED SURFACES : *A Multi-scale Analysis of the Touch-up Problem*

A Thesis

Submitted in Partial Fulfillment of the

Master of Science in Industrial Engineering

in the

Department of Industrial & Systems Engineering

Kate Gleason College of Engineering

By

Suparna Kishore Kalghatgi

February, 2011

DEPARTMENT OF INDUSTRIAL & SYSTEMS ENGINEERING

KATE GLEASON COLLEGE OF ENGINEERING

ROCHESTER INSTITUTE OF TECHNOLOGY

ROCHESTER, NEW YORK

CERTIFICATE OF APPROVAL

M.S. DEGREE THESIS

The M.S. Degree Thesis of Suparna Kishore Kalghatgi
has been examined and approved by the
Thesis Committee as satisfactory for the
Thesis requirement for the
Master of Science degree

Approved by:

_____

Dr. Marcos Esterman, Thesis Advisor

_____

Dr. James A. Ferwerda

_____

Dr. Matthew M. Marshall

ACKNOWLEDGEMENTS

I would like to express my heartfelt gratitude towards my entire thesis committee- Dr. James A. Ferwerda for his guidance, teaching and encouragement throughout the course of this thesis; Dr. Marcos Esterman for his words of advice; and Dr. Matthew Marshall for his recommendations and valuable suggestions.

I am thankful to Dr. Jonathan Arney, Dr. Susan Farnand and Dr. David R. Wyble, for their help with the BRDF and surface topography measurements; and Dr. Koichi Takase, Dr. Tongbo Chen and Lawrence Taplin, for their assistance in developing the code for normal map estimation.

My fellow members of the 3D Imaging Group at the Munsell Color Science Lab - Benjamin Darling, Dan Zhang and Jonathan Phillips, have played a very significant role towards the successful completion of this project. I thank them for their immense contribution in developing the code used for the modeling and rendering of the synthetic images and for the psychophysical experiments.

I would like to gratefully acknowledge Sherwin Williams Paints for funding this project, and our company advisors- Paul H. Kayima, Shermila B. Singham and Mary E. Tuel for their invaluable input at every stage of this research.

Lastly, I would like to recognize my parents- Kishore and Alka Kalghatgi, and my sister Pallavi. It is their unconditional love, support and faith in me that has enabled me to complete my Masters program successfully. I dedicate this thesis to them.

Thank you all very much!

ABSTRACT

Real-world surfaces typically have geometric features at a range of spatial scales. At the microscale, opaque surfaces are often characterized by bidirectional reflectance distribution functions (BRDF), which describes how a surface scatters incident light. At the mesoscale, surfaces often exhibit visible texture – stochastic or patterned arrangements of geometric features that provide visual information about surface properties such as roughness, smoothness, softness, etc. These textures also affect how light is scattered by the surface, but the effects are at a different spatial scale than those captured by the BRDF. Through this research, we investigate how microscale and mesoscale surface properties interact to contribute to overall surface appearance. This behavior is also the cause of the well-known "touch-up problem" in the paint industry, where two regions coated with exactly the same paint, look different in color, gloss and/or texture because of differences in application methods.

At first, samples were created by applying latex paint to standard wallboard surfaces. Two application methods- spraying and rolling were used. The BRDF and texture properties of the samples were measured, which revealed differences at both the microscale and mesoscale. This data was then used as input for a physically-based image synthesis algorithm, to generate realistic images of the surfaces under different viewing conditions. In order to understand the factors that govern touch-up visibility, psychophysical tests were conducted using calibrated, digital photographs of the samples as stimuli. Images were presented in pairs and a two alternative forced choice design was used for the experiments. These judgments were then used as data for a Thurstonian scaling analysis to produce psychophysical scales of visibility, which helped determine the effect of paint formulation, application methods, and viewing and illumination conditions on the touch-up problem. The results can be used as base data towards development of a psychophysical model that relates physical differences in paint formulation and application methods to visual differences in surface appearance.

TABLE OF CONTENTS

LIST OF FIGURES

LIST OF TABLES

1 MOTIVATION

Visual appearance of a surface is important to most industries. Surface appearance is evaluated in terms of attributes or specific visual qualities of the object, such as hue, saturation, shape, roughness, gloss, transparency etc. These various appearance features can be broadly classified into two categories- those associated with color and those that result from their geometric attributes.

Real-world surfaces typically have geometric features at a range of spatial scales. At the microscale, opaque surfaces are often characterized by bidirectional reflectance distribution functions (BRDF), which describes how a surface scatters incident light. At the mesoscale, surfaces often exhibit visible texture – stochastic or patterned arrangements of geometric features that provide visual information about surface properties such as roughness, smoothness, softness, etc. These textures also affect how light is scattered by the surface, but the effects are at a different spatial scale than those captured by the BRDF. Through this research, we investigate how microscale and mesoscale surface properties interact to contribute to overall surface appearance.

In the commercial paint industry, the interaction between the microscale and mesoscale surface properties is the cause of the well-known "touch-up problem", where two coats of the same paint, a base coat and a top, touch-up coat, look different in appearance. The touch-up problem may manifest itself as differences in color, gloss and/or texture between the base and touch-up regions and the differences can vary with surface illumination and viewing conditions.

Figure 1 demonstrates the touch-up problem. The left panel shows a wall in an office hallway that was spray painted with a base coat of matte white paint. Over time, scratches and defects appeared on the wall surface and a touch-up coat of the same paint was applied locally with a fabric roller. When the wall is viewed straight on, the base and touch-up regions match reasonably well. But when the wall is viewed obliquely, with grazing illumination (as might happen in natural viewing conditions), the base and touch-up regions differ significantly in

appearance, revealing the repairs and reducing the perceived quality of the repair job. In architectural applications, the touch-up problem is a significant and costly problem for both the paint and construction industries. The problem can be extended to other industries as well, such as automotive manufacturing and repair.

Figure 1: The touch-up problem. The left panel shows a section of a white, matte painted wall viewed straight-on. The right panel shows the same wall section viewed obliquely. Note the differences in surface lightness and gloss in the base and touched-up region.

The goal of this research is to conduct multiscale analysis of the touch-up problem and derive quantitative information about the material parameters that must be controlled to minimize this effect in painted surfaces. Measurement of the surface's reflectance and surface properties can enable modeling of the surface appearance under different lighting and viewing conditions. Psychophysical analysis of these renderings can then help generate models for predicting changes in appearance. The overall goal of the project is to derive a psychophysically based light reflection model that is capable of accurately predicting the visual appearance of the painted surface from physical measurements of their reflectance properties. This will enable systematic analysis of formulations and application techniques to help minimize the touch-up effect.

2 BACKGROUND

The focus of this research is to develop a comprehensive understanding of the touch-up problem in the paint industry, and the steps that can be taken to minimize it. The background section begins with some basic information on paint, its properties and the application methods commonly used in commercial applications. In order to understand the touch-up behavior, the first step is to investigate the physical and visual factors that contribute to it. In order to do so, we need to understand the surface properties that govern appearance. At the microscale level, the appearance of a surface is described using the bi-directional reflectance distribution function (BRDF) which describes how a surface scatters incident light. The mesoscale texture is manifested in the form of differences in visual appearance of surface roughness. The observed variation in perceived surface appearance is caused by the interaction between the microscale and mesoscale texture. Hence the second part of this section describes different methods used to measure these surface properties.

Next, the BRDF and texture data is used as input for a physically-based image synthesis algorithm to generate realistic images of the surfaces under different viewing conditions. The third part of this section contains a brief overview of the different BRDF models that are commonly used for computational modeling of the surfaces and the different methods used for generating physically accurate renderings of the surfaces using computer graphics techniques.

Finally, in order to gain a complete understanding of the touch-up effect, it is important to determine the factors that have the greatest influence on this effect. The touch-up effect is a visual problem and can depend on both the surface properties and application methods or on the environmental conditions. The approach typically followed to do this is to correlate the surface properties to an observer's judgment of differences in visual appearance. This is done using psychophysical testing. Images of samples at various lighting and viewing conditions can be used as stimuli for these experiments. The last section gives an overview of the concept of psychophysics and the most common methods used to conduct experiments.

2.1 PAINT

Paint is a ubiquitous material in the build environment. Paint serves as a surface finish for a wide range of materials, including wood, stone, metal, paper etc. Many different kinds of paint have been created including oil-based alkyds, water-based latex, acrylics, tempera and encaustics. All paints typically consist of the following components: pigment, binder, solvent and additives.

(i) Pigment: Pigments are granular solids incorporated into the paint to contribute color, toughness or texture to the paint. Most commonly used pigments are clays, calcium carbonate and silicas.

(ii) Binder: This is the actual film forming component of paint. The binder imparts adhesion and binds the pigments together. It strongly affects properties such as gloss potential, exterior durability, toughness and roughness.

(iii) Solvent: The main purpose of the solvent is to adjust the curing properties and viscosity of paint. It controls the flow and application properties.

(iv) Additives: Paints can have a wide range of miscellaneous additives which are added in small quantities but impart very significant effects. Additives are usually used to modify surface tension, improve finished appearance, control foaming, anti-freeze properties etc.

Two main factors affect paint appearance: formulation and application

2.1.1 PAINT FORMULATION

Although paints differ widely in the components used in their formulation, they all consist of pigment particles suspended in some kind of liquid binder. Differences in particle and binder properties lead the wide variations in color and gloss seen in different kinds of paints. Unusual formulations can also be used to produce “special effects” such as metallic sparkle, luster, surface crinkle and goniochromatic shifts.

2.1.2 PAINT APPLICATION

The other main factor affecting the appearance of painted surfaces is the method of application. The classic method is with a brush, and different types of brushes can produce relatively smooth surfaces or ones with significant relief or “impasto”. In architectural construction popular application methods include airless spraying and use of a fabric roller. Spraying is a very efficient application technique for covering large areas. Spraying is a method of applying the paint at a very high pressure so as to atomize it. This is done by forcing the paint through a small opening at a very high pressure. The main components of an airless sprayer are a pump, hose, gun and a tip. This technique is very efficient for covering large areas. Also, a uniform coating of any desired thickness can be applied. Due to the fine drop size and random drop distribution, it tends to produce surfaces with a uniform “noisy” texture. Hence, this method is more commonly used for applying the base coats on drywall surfaces (House-Painting-Info.com, 2009). On the other hand, a major disadvantage of this method is that spray-painting tends to bridge small cracks and does not fill them up completely. This is especially a problem on a newly textured drywall. To eliminate this problem, a second method called rolling is employed. Rolling is a simple method for that requires minimal equipment and depending on the nap of the roller can produce finishes with a wide range of textures from fine to large scale. Backrolling is a hybrid technique in which the paint is applied with a spray gun, but then the wet paint is rolled to finish the surface. In the construction process spraying is often used to apply a base coat, and then backrolling is used to touch-up any defects.

2.1.3 RELATIONSHIP BETWEEN PAINT APPEARANCE EFFECTS AND SPATIAL SCALES

As a material paint seems homogeneous and simple, but this simplicity hides complex chemical, physical and optical properties, and the final appearance of a painted surface depends on processes that occur in different modalities at many spatial scales. This is illustrated in Figure 2.

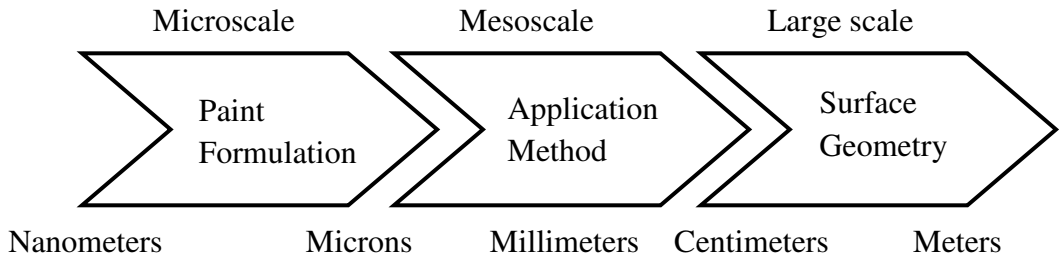

Figure 2: Diagram showing the relationships between the paint appearance effects and spatial scale

At the finest (nanometer/micron) scale there are the reflectance properties of the pigment particles that affect both spectral and directional light scattering at the microscale. As the paint dries and the binder evaporates, particle shape also comes into play affecting how the particles aggregate on the surface. At the mesoscale (~millimeters) paint application methods such as spray or rolling, and the texture of the substrate comes into play, affecting the thickness and relief of the paint surface. Finally large-scale surface geometry (~centimeters/meters) can also play a role, with paint coats forming differently on flat, curved, horizontal and vertical surfaces.

2.2 MEASUREMENT OF REFLECTANCE AND TEXTURE

When light is incident on a surface, it penetrates the sample, scatters spatially and angularly and then returns to the surface as reflected light. The former is known as “diffuse light” and the latter is called “angularly distributed specular light”. The diffuse light is predominantly responsible for the color of a sample whereas the specular light contributes to the gloss effects (Arney, et al., 2004). The specular light is distributed over many angles and the Bidirectional Reflectance Distribution Function (BRDF) is used to describe the distribution of light around the specular direction (Arney, Ye, et al., 2006). When an instrument is used to measure gloss, it needs to separate the diffuse light from the specular light reflected off of a given sample.

Object appearance is directly related to the geometric conditions of viewing, that is, the direction of illumination and view. To observe color, a viewer avoids the specular reflection since the glossiness masks the color. Therefore, a diffuse angle of viewing, such as 0° when light is incident at 45°, is used. On the other hand, if glossiness is to be assessed, the observer should view the sample at an equal and opposite angle of reflection (Hunter & Harold, 1987). This is the principle of working of gloss measuring devices.

2.2.1 SURFACE REFLECTANCE MEASUREMENT

Gloss meters are the most commonly used devices used to measure characteristics of specular light reflected from materials. They measure gloss on the basis of illumination and detection at equal and opposite angles as shown in Figure 3 and provide measurement of gloss on the basis of a gloss index, G.

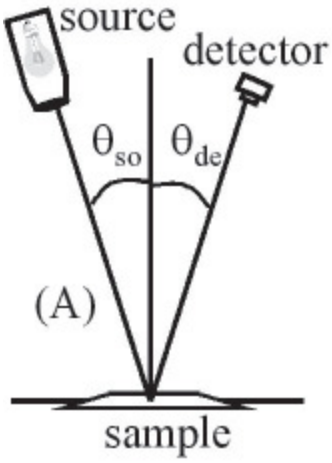

Figure 3: Illumination angle θ_{so} and detection angle, θ_{de} are equal and opposite in glossmeters (Arney, Peter, & Hoon, 2004)

Gloss meters separate the specular light from the diffuse component by measuring only at the peak of the BRDF where specular light is concentrated and diffuse light is negligible by comparison. This does not give a very accurate representation of the gloss of a surface (Arney, et al., 2004). The underlying material properties that are related to the gloss of a surface are the refractive index, the absorption coefficient and the distribution of surface facet angles (Arney & Nilosek, 2007). But the relationship between G numbers and the corresponding properties of the materials is still not completely clear (Arney, Ye, et al., 2006). Surface roughness is also known to affect gloss meter measurements. An increase in surface roughness results in reduced gloss because the roughness disperses the specular light about the specular angle, θ (Arney, Ye, et al., 2006).

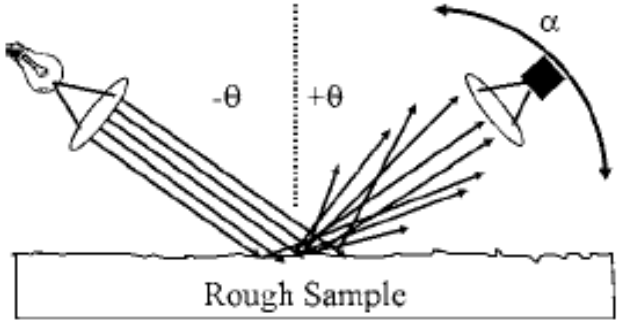

Figure 4: Roughness distributes the specular light around the specular direction and decreases gloss (Arney, Ye, & Banach, 2006)

This translates instrumentally to an increase in the measured angular distribution of specular light (Arney, et al., 2004). Gloss meters are not equipped to measure such angular distributions effectively.

Significantly more information about gloss can be obtained from the bi-directional reflectance distribution function (BRDF) measured by detecting light reflected at angles beyond the equal and opposite specular angle (Arney, Jiff, Oswald, & Ye, 2006). This is done using a goniophotometer which measures the reflected light as a function of angle of detection θ_{de}, angle of source illumination θ_{so} or angle of tilt of the sample α. The BRDF obtained is a graph of the average irradiance, I, as a function of θ_{de}, θ_{so} or α (Arney, et al., 2004). This is illustrated in Figure 5.

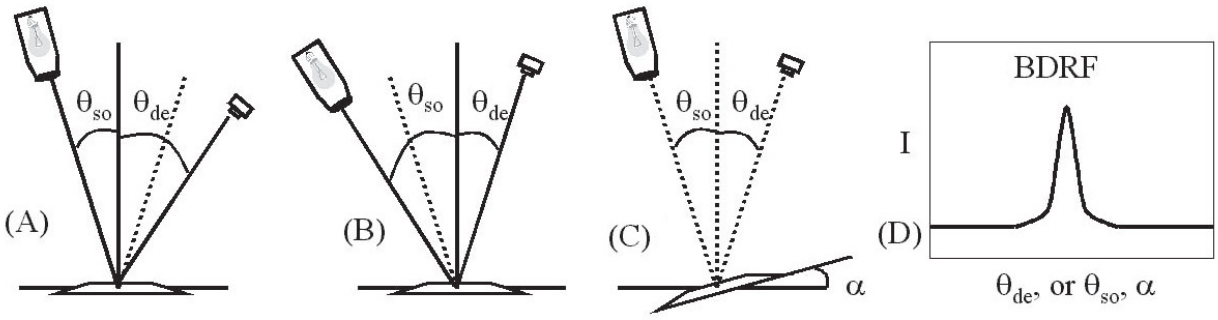

Figure 5: A goniophotometer measures the reflected light as a function of (A) the angle of detection θ_{de}; (B) the angle of illumination θ_{se}; and/or (C) the angle of tilt of the sample, α. Each produces a bi-directional reflectance factor function, BRDF, illustrated in (D) (Arney, et al., 2004)

If the incident and reflected flux on a surface is considered, the bi-directional reflectance distributed function is defined as the ratio of directional reflected radiance to the directional incident radiance. The BRDF is denoted by the symbol f_r and is represented by the equation given below (Nicodemus, Richmond, Hsia, & Ginsberg, 1977).

$$f_r(\theta_i, \phi_i; \theta_r, \phi_r) = dL_r(\theta_i, \phi_i; \theta_r, \phi_r; E) / dE_i(\theta_i, \phi_i) \, (\mathrm{sr}^{-1})$$

In the above equation, the subscript *i* indicates incident radiant flux whereas *r* indicates reflected radiance flux. Table 1 explains the symbols related to the BRDF (Chen, 2008)

Symbol	Term	Unit Dimension
Θ	Polar Angle	[rad]
Φ	Azimuth Angle	[rad]
E	Irradiance	[Wm^{-2}]
L	Radiance	[$Wm^{-2}sr^{-1}$]
dω	Solid Angle	[sr]
dA	Surface Element	[m^2]

Table 1: List of symbols related to the BRDF

Figure 6 depicts the BRDF in terms of illumination and viewing angles. In this case, a surface element (dA) is illuminated from the incident direction (θ_i, φ_i) within solid angle ($d\omega_i$), with reflection taking place in the direction (θ_r, φ_r) within the solid angle ($d\omega_r$)

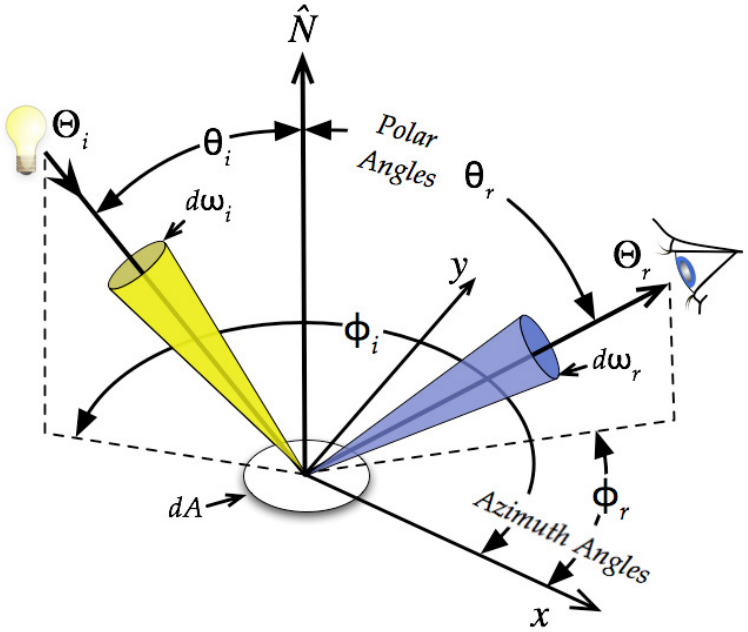

Figure 6: BRDF expressed in terms of viewing and illumination angles (Chen, 2008)

2.2.2 MEASUREMENT OF SURFACE TOPOGRAPHY

Since the 15th century, artists have applied the laws of geometric perspective to represent three-dimensional space and shape in two-dimensional images. A number of tools have been used to characterize shapes and topography. Significant information about the visual appearance of a surface can be derived from measures of its topographic features. Photometric stereo is an image-based technique for measuring surface topography that comes from the field of computer vision.

In the photometric stereo method, the surface orientation is determined from two or more images by using their corresponding reflectance maps. A reflectance map determines image intensity as a function of its surface gradients. It represents the surface reflectance of a material for a particular light source, object surface and viewer geometry. Reflectance maps are determined empirically, from phenomenological models of surface reflectivity or derived from analytical models of surface microstructure. The reflectance map is also related to the bi-directional reflectance distribution function (BRDF) of a material.

The idea of photometric stereo is to vary the direction of incident illumination between two successive views, keeping the direction of viewing constant. Since there is no change in the imaging geometry, each picture element in the images obtained correspond to the same object point and hence to the same gradient. The varying of the direction of incident illumination only varies the reflectance map that characterizes the imaging situation. A combination of these maps can be used to determine the surface orientation at each image point.

The photometric stereo method is famous because of its simple yet effective methodology. The only computation required is for the initial determination of the reflectance map for each experimental situation. Since images are obtained from the same point of view, it is easy to identify corresponding points in the images. This reduces a lot of the computation involved in traditional stereo. The multiple images required for

photometric stereo can be obtained by moving a single light source or my using multiple light sources calibrated with respect to each other, or by rotating the object surface and imaging hardware together to stimulate the effect of moving a single light source. Photometric stereo works best on smooth surfaces with uniform surface properties (Woodham, 1980).

A simplified application of the photometric stereo method is used by museum professionals to examine works of art on paper is the raking light method, where the texture and topography is documented by observing and photographing the object illuminated with a light source placed at a low angle , measured from the horizontal plane of the object (Arney & Stewart, 1993).

As illustrated in Figure 7, the topography of a surface is described as a variation in the height h(x) across the paper, where x is the dimension in the direction of illumination. This also means that the topography is described as a variation of the tilt angle α(x) across the surface.

$$d[h(x)]/dx = \tan[\alpha(x)]$$

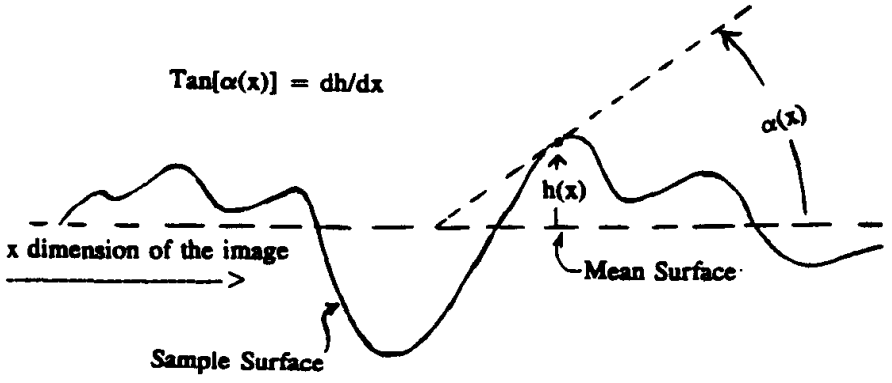

Figure 7: Schematic representation of the relationship between topographic height, h, and the surface angle, α (Arney, Tantalo, & Stewart, 1994)

The setup used for image capture using the raking light method is illustrated in Figure 8.

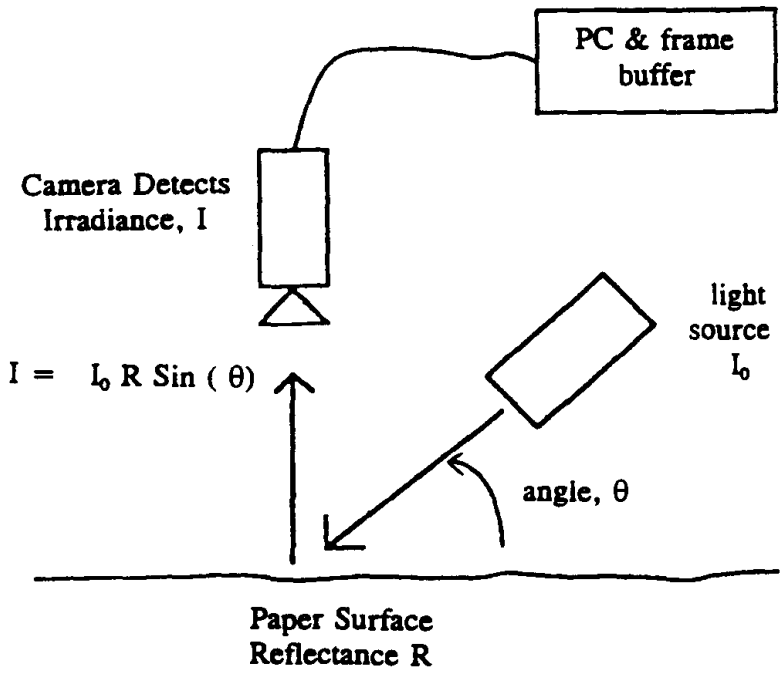

Figure 8: Geometry of "raking angle" illumination and image capture for the characterization of surface topography

The sample is placed in the horizontal plane and is illuminated by a regulated light source mounted on an arm that can be set at any angle of illumination, θ, between 0° and 90°, relative to the plane of the sample. A camera is used to detect the irradiance, which is recorded on a computer. Typically, images are captured of the sample, when it is illuminated at equal and opposite angles of illumination. One of the assumptions made in this method is that the sample behaves as a Lambertian reflector, which means that the material scatters light and appears to have constant brightness, regardless of the angle of viewing. This implies that the irradiance detected by the camera is not a function of the angle of viewing of the camera. However, the angle of illumination, θ is directly related to the apparent brightness of the object as detected at the camera, I, and the reflectance factor across the surface. Thus, in order to generate the topographical height h(x), the experimentally observed variations in the pixel values of the two images are examined and the values of tan[α(x)] are extracted. Pixel by pixel integration of this data can produce topographical height h(x) (Arney, et al., 1994).

2.3 SURFACE MODELING AND RENDERING

Computer graphics image synthesis techniques offer a powerful set of tools for studying surface appearance. Over the past thirty years computer graphics modeling and rendering methods have developed from creating crude representations of simple geometric shapes to being able to produce radiometrically accurate simulations of surfaces with complex shapes, textures and material properties situated in rich natural lighting environments (Greenberg, 1997). The basic image synthesis pipeline is illustrated in Figure 9.

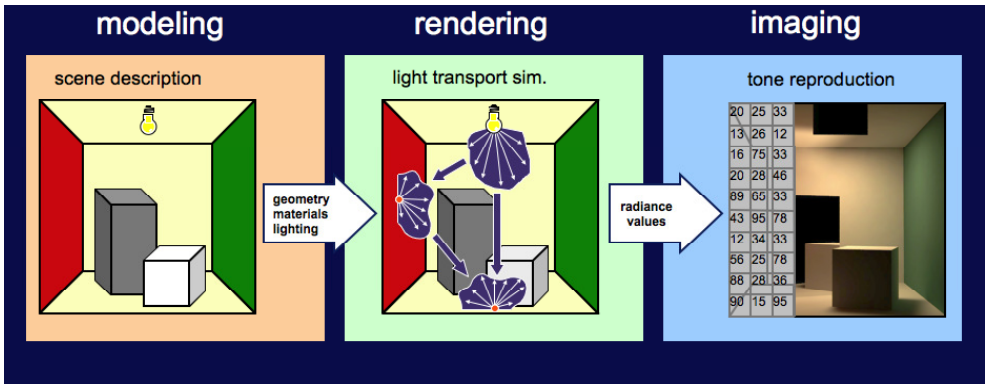

Figure 9: The image synthesis pipeline (after (Greenberg, 1997)

The entire process is organized into three parts- the first dealing with the local light reflection model, the second dealing with the global light transport simulation and finally, the image display. For the first stage, an accurate physically based light reflection model is derived for arbitrary reflectance functions. In the next stage, the rendering algorithms accurately simulate the physical propagation of light energy throughout the modeled environment. Once accurate results are obtained in the first two stages, the third stage is reached, which deals with the creation of accurate images perceptually.

2.3.1 LIGHT REFLECTION MODELS

In the modeling stage, a mathematical model of the scene is created by describing the 3D surface geometry, surface reflectance properties and emissive properties of the light sources. Material properties are described using light reflection models such as the Phong

(Phong, 1975), Ward (Ward, 1992), or Cook-Torrance (Cook & Torrance, 1981) models that parameterize surface BRDFs. Given a light source, a surface and an observer, a reflectance model describes the intensity and the spectral composition of the reflected light reaching the observer. This is determined by the intensity of the light source and the reflecting ability and surface properties of the material.

2.3.1.1 EMPIRICAL MODELS

Empirical or phenomenological models use a combination of functions to capture all the features of reflection that are commonly observed, such as diffuse reflectance in all directions and concentration of light scattering in a near specular direction for glossy materials. Empirical models do not simulate reflection or scattering from basic laws of physics. They typically consist of mathematical functions that can be controlled by a small number of parameters.

Lambertian or "ideal diffuse" reflectance is the condition where all light instead of being reflected in a single direction (specular reflection), is reflected in all directions with the same radiance. Real materials usually deviate from Lambertian for angles of incidence greater than 60°, but this model is used for its computational simplicity.

One of the simplest empirical models was proposed by Phong in 1975 (Phong, 1975). Only two parameters describe the specular component in this model. This model is popular because of its mathematical simplicity.

The Ward model introduced in 1992 is similar to the Phong model. Ward developed the imaging gonioreflectometer at the Lawerence Berkeley Laboratory. His model was derived by fitting the imaging data obtained from this instrument (Ward, 1992). The main advantages of this model are that it uses only a few simple parameters making it easier to control, it can be sampled efficiently for Monte Carlo and can model anisotropic surfaces (Walter, 2005).

In 1997, Lafortune developed a BRDF model using non-linear parameters for light reflection functions. His model was able to capture off-specular reflection, increasing reflectance and retro-reflection (Lafortune, Foo, Torrance, & Greenberg, 1997)

2.3.1.2 PHYSICALLY BASED MODELS

Physically based models are also called "first principles" models. They are developed based on the theory of optics and physics applied to a surface's microscopic structure. Thus every parameter in the model represent either the characteristic of the material or its physical behavior (Chen, 2008).

The first step in developing analytical models is modeling the surface geometry at the microscopic level. Torrance and Sparrow developed a light reflection model for roughened surfaces in 1967. This model assumed that the surface area was comprised of small, randomly dispersed, mirror-like facets. This model also contained a term that helped to analyze the shadow and masking phenomena. The model helped explain off-specular peaks that occur when the angle of incidence increases away from the surface normal (Torrance & Sparrow, 1967).

Blinn further improved the performance of this model and introduced it to computer graphics (Blinn, 1977). Blinn selected a distribution developed by Trowbridge and Reitz that modeled the micro-facets randomly oriented and randomly curved. This model was more accurate than the other models, resulting from better fitting to the measured data.

Cook and Torrance developed a more generic reflection model to describe the directional distribution of the reflected light and a color shift that occurs as the reflectance changes with incident angle (Cook & Torrance, 1981). Multiple distribution functions were included in this model for the distribution of the micro-facets.

The Oren-Nayar model was an extension of the Cook-Torrance model that assumed Lambertian instead of mirror reflection at the facet level (Oren & Nayar, 1995). This

model was able to predict backscattering, which occurs when facets oriented towards the light source diffusely reflect some light back to the source. The Blinn and Cook-Torrance models do not explain backscattering whereas the Oren-Nayar model does not give off-specular peaks, therefore these models are often used together to produce the full BRDF.

2.3.2 RENDERING

The light reflection model gives the emission, geometry and reflection functions. Once these are known, in the rendering stage the model serves as input to a light transport algorithm that simulates how light propagates through the scene. Any point in a scene can either receive direct light from illumination sources or receive indirect illumination from surface inter-reflections (Macey, 1997). Tracing every particle of light is nearly impractical and would require a large amount of computation time. Therefore, four categories of light transport modeling have emerged, which are described in brief below.

2.3.2.1 RASTERIZATION

Rasterization is the task of taking an image described in a vector graphics format (in the form of shapes) and converting it to a raster image (in the form of pixels or dots) for output or storage in the form of an image. The most basic algorithm for this method takes a 3D scene, described in the form of polygons, and renders it onto a 2D surface, usually a computer monitor (Wiley, Romney, Evans, & Erdahl, 1967). Though rasterization is one of the fastest rendering techniques, it is largely based on artistic intent and hence is not a very accurate technique for computer graphics.

2.3.2.2 RAY CASTING

In ray casting, once the geometry of the scene is modeled, it is parsed pixel by pixel from the point of view (eye) outwards, as if casting rays out from the point of view. The idea is to find the closest object blocking the path of that ray. Using the material properties and the effect of lights in the scene, the algorithm can determine the shading of this object.

Ray casting is used primarily for realtime simulations where detail is not highly important and can be easily approximated in order to achieve better computational speed (Macey, 1997). The resulting surfaces have a characteristic "flat" appearance, if no advanced rendering techniques are used.

2.3.2.3 RAY TRACING

In computer graphics, ray tracing is a commonly used method to generate an image by tracing a path of light through pixels in an image plane and simulating the effect of its encounters with virtual objects (Nikodym, 2010). Ray casting algorithms cast rays from the eye into the scene but the rays were traced no further. Ray tracing follows the ray of light even after it has encountered a surface, which causes a more realistic simulation of lighting. Effects such as reflections and shadows are a natural outcome of the ray tracing algorithm when Monte Carlo methods are applied to it. A major disadvantage of ray tracing however, is computational cost and performance (Macey, 1997).

2.3.2.4 RADIOSITY

Radiosity is a method which attempts to simulate the way in which directly illuminated surfaces act as indirect light sources that illuminate other surfaces. This is also called as diffuse interaction. It uses the finite element method to solve the rendering equation for scenes with purely diffuse surfaces. The inclusion of radiosity calculations lends an element of added realism to the scene because of the way it mimics real world phenomena. The advantage of radiosity methods is that once the illumination of a scene is computed, the results are independent of the observer's position. Therefore, radiosity is often used as a supplement to ray tracing methods in order to enhance the rendered scene (Goral, Torrance, Greenberg, & Battaile, 1984).

2.3.3 IMAGING

Generating a visual image is the final stage of realistic image synthesis. A major goal of this stage is to create an image that is perceptually indistinguishable from the actual scene. At the end of the light transport process, radiometric values at every point of the 3D scene are known. In the imaging stage, the simulated scene radiances are mapped to produce a visual image. It has to account for the physical parameters of the display being used, the perceptual characteristics of the observer and the conditions under which the scene will be viewed. Most physically based rendering methods described in the section above are able to accurately simulate the physical behavior of light. But this does not guarantee that the images developed will have a realistic visual appearance. The first reason for this is the limitation of display devices in terms of resolution, luminance range and color gamuts. Secondly, the scene's observer and display observer may be in different visual states, affecting their perception of the displayed visual scene.

There are limits on the fidelity of display devices. Tone and gamut mapping are some of the techniques used to overcome these limitations. Tone mapping is a technique used in computer graphics to map one set of colors to another, to approximate the appearance of high dynamic range images in a medium that has a limited dynamic range (like monitors). Most devices also do not have the same subset of colors which can be accurately represented on a display device, also called gamut. Gamut mapping is a technique for transforming the colors of a source image into the color space of the display device that best reproduces the appearance of the source. These techniques can help achieve a greater perceptual match between a real scene and displayed scene, even though the display device is not able to reproduce the full range of luminance and color values.

Improving the visual realism of synthetic images is a still underexplored area of computer graphics. In order to produce realistic images, one needs to model not only the physical behavior of light, but also the parameters of perceptual response. This is done by modeling the transformations that occur in the brain during visual processing. The goal is often to

produce an image that accurately represents the visual appearance of the scene from a human observer's point of view (Greenberg, 1997).

2.4 PSYCHOPHYSICS

Psychophysics is a branch of psychology that deals with human responses to physical stimuli, particularly related to the perception of human magnitude. It is described as the "scientific study of the relation between stimulus and sensation" (Gescheider, 1997).

In the commercial industry, appearance of an object is an importance factor contributing towards customer satisfaction. Most commonly, the emphasis for the study of appearance has been on an objective evaluation which involves physical measurement of images. But at the same time, it is important to also study subjective appearance evaluation, which focuses on collecting and analyzing judgments from human customers. Customer perceptions are the visual perceptual attributes that form the basis of the quality preference of judgment by the customer. The purpose of the psychophysical experiments is to assign numbers to these attributes. Most psychophysical experiments either involve determination of thresholds or formulating a psychophysical scale (Engeldrum, 2000).

2.4.1 DETERMINATION OF THRESHOLDS

A threshold is the point of intensity at which a participant can just detect the presence of, or difference in, a stimulus. Presenting a stimulus to observers and asking them to report whether or not they perceive it is the basic procedure for measuring thresholds. Some of the classical methods for stimulus detection or difference detection are described in brief below (Guilford, 1954).

(i) Method of Limits: This is the most common technique for determining sensory thresholds. The experimenter initially presents a stimulus well above or well below the threshold level. On each successive presentation, the threshold is approached by changing the stimulus intensity by a small amount until the boundary of sensation is reached. The manipulation can be done in either an ascending or descending manner.

(ii) Method of Constant Stimuli: In this process, the same set of stimuli is repeatedly used throughout the experiment. The property being varied is not related from one

trial to the next, but is presented randomly. This prevents the subject from being able to predict the level of the next stimulus. The 50% threshold is located somewhere within the range of stimulus values.

(iii) Method of Adjustment: The method of adjustment asks the subject to alter the level of the stimulus until it is barely detectable against the background noise or is the same as the level of another stimulus. The difference between the variable stimuli and the standard one is recorded after each trial.

2.4.2 PSYCHOPHYSICAL SCALING

Although the investigation of sensitivity by measuring absolute and difference thresholds provides valuable information about the senses, it does not give a complete picture of the system. Psychophysical scaling methods differ from the traditional methods in that the end results are not values on physical scales but are on psychophysical scales. Some of the most commonly used psychological scaling methods are described in brief.

(i) Method of Pair Comparisons: In this method of pair comparisons, all stimuli to be evaluated on a psychological scale are typically presented to the observer in all possible pairs. The observer judges whether one of the pair is of greater quantity than the other in some defined respect. L. L. Thurstone first introduced a scientific approach to using pairwise comparison for measurement in 1927, which is called the Thurstone Law of Comparative Judgment. He demonstrated that the approach could be used to order items along a dimension such as preference or importance, using an interval-type scale (Guilford, 1954).

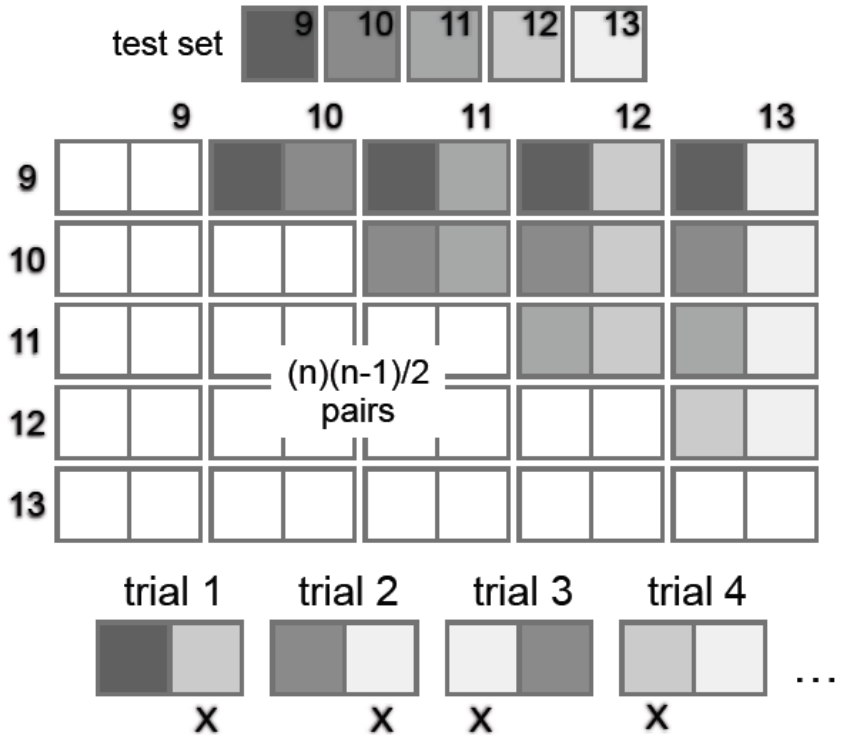

Figure 10: Experimental set-up for Method of Paired Comparison

(ii) Method of rank order: This method is popular because of the ease with which large number of stimuli can be judged with reference to each other. It forces observers to make the maximum number of discriminations and thus provides as much information as is possible to obtain from them. Hence this method is similar to a simultaneous pair comparison method. Any stimuli that can be manipulated in any manner so that an observer can place them in serial order (from dark to bright, or rough to smooth), can be analyzed using this method. All the stimuli in this method are present for simultaneous observation.

(iii) Category Scaling: This method required observers to place stimuli in categories which may be labeled with names such as “good”, “better and “best” or with numbers.

(iv) Multidimensional scaling: Multidimensional scaling is a statistical method for finding the latent dimensions in a dataset. Its most common applications are in data mining in fields such as cognitive science, psychometrics, etc. Typically, potential customers are asked to compare pairs of products and make judgments

about their similarity or dissimilarity. MDS then obtains the underlying dimensions from respondents' judgments about their similarity and reconstructs a space that explains the dataset's overall structure (Gescheider, 1997).

2.5 SURFACE APPEARANCE CHARACTERIZATION

As described in Section 1, visual appearance is evaluated using two broad categories of attributes- those associated with color and those that result from the geometric attributes of a surface. These geometric attributes can further be classified as gloss and texture, which describe the spatial distribution of light at the microscale and mesoscale respectively.

2.5.1 COLOR

Color can be considered to be a composite, three-dimensional characteristic consisting of a lightness attribute and two chromatic attributes called hue and saturation. Color is related to a surface's spectral reflectance properties. Many models have been developed for describing color. The simplest one is the RGB model used in video and computer graphics. The more sophisticated ones are Munsell, XYZ, CIELAB etc. which have the psychophysics of color perception as their basis (Hunter & Harold, 1987).

2.5.2 GEOMETRIC ATTRIBUTES

Surfaces can be analyzed at various spatial scaled. Variations at the microscale level include changes in the microscopic surface structure. This variation causes a difference in the spatial distribution of light by the object and is called gloss. Gloss depends on a surface's directional reflectance properties. It cannot uniquely be described by an organized coordinate system. If a surface is to be completely described, another important aspect of its appearance is texture, or the "bumpiness" of the surface. Significant information about the visual appearance of a surface can be derived from the measures of its topographical features.

Most models used to describe gloss are based on quantitative studies of light reflection and though very accurate, the parameters used in these models are unintuitive and do not describe gloss appearance. Hence, there is a need to develop a gloss model that is based

on the physics of light reflection and at the same time, considers the phenomenology of gloss perception (Hunter & Harold, 1987).

According to the classic work done by Hunter in 1936, there are around six different visual phenomena related to apparent gloss (Hunter & Harold, 1987). They are:

(i) Specular Gloss: Perceived surface brightness associated with the specular reflection from a surface
(ii) Sheen: Perceived shininess at grazing angles seen in otherwise matte specimens
(iii) Distinctness of Image (DOI) Gloss: The sharpness with which images are perceived after reflection from a surface
(iv) Contrast Gloss (Luster): Perceived relative brightness of brighter and less-bright areas adjacent to each other on the surface of an object. This takes place because of selective reflection in directions relatively far from those of specular reflection.
(v) Reflection Haze: Perceived scattering of light (cloudiness) reflected from a surface in directions near those with specular reflection.
(vi) Absence-of-texture Gloss: Perceived surface smoothness and uniformity.

Judd (Judd, 1937) used Hunter's observations to formulate expressions that related the types of gloss to the physical features of surface bi-directional reflectance distribution functions (BRDFs). Hunter and Judd's research is important because it was one of the first to recognize the multi-dimensional nature of gloss perception. Their research has been used as a framework for all other work related to gloss perception. However, it is not always easy to correlate their metrics with object appearance under natural conditions (O'Donnel, 1984).

One of the significant works in the field of gloss perception was done by Billmeyer and O'Donnell, who tried to address this issue from first principles (O'Donnel & Billmeyer, 1986). They used a set of white, gray and black paints with varying gloss levels and collected ratings of perceived differences in gloss between pairs of samples. They then used multi-dimensional scaling techniques to derive the dimensionality of apparent gloss.

Their samples were flat and were viewed under direct illumination with black surround. From their experiments, they concluded that the appearance of high gloss surfaces is best described by what Hunter calls distinctness-of-image gloss, and the appearance of low gloss surfaces is best described by contrast gloss. The only limitation of their work was that they look at surfaces under uniform surrounds, whereas in order to study perception of gloss, we need to study objects in realistically rendered environments.

(Ferwerda, 2001) use image synthesis techniques to explore the relationship between physical dimensions of gloss reflectance and perceptual dimensions of gloss. They used a set of achromatic glossy paints to conduct two experiments. In their experiments, they use multidimensional scaling to determine the dimensionality of gloss perception and create a perceptually uniform "gloss space". They inferred that gloss has two dimensions, which are qualitatively similar to the contrast gloss and distinctness-of-image gloss as described by Hunter. Their work is significant as it attempts to develop a psychophysically-based light reflection model where the dimensions of the model are perceptually meaningful and the variations along the dimension are uniform. They also use this model to describe surface appearance in graphics rendering applications.

3 EXPERIMENTS

The touch-up effect is essentially a visual problem. Touch-up visibility can broadly depend on surface properties or environmental conditions. Surface properties are governed at the microscale by the reflectance of the surface and at the mesoscale, by the surface texture. In practical terms, these are interlinked with the paint formulation and application methods. Environmental conditions include the lighting and viewing conditions prevalent in the surroundings. Modifying these environmental factors can increase or decrease the perceptual magnitude of the touch-up problem.

In order to develop an understanding of the factors that have the greatest influence, it was necessary to first perform a qualitative analysis of the touch-up problem. This was done using two psychophysical experiments aimed towards determining the effect of the various surface and environmental conditions on the visibility of the touch-up region.

3.1 SAMPLE PREPARATION

The first step to performing the psychophysical experiments was creation of touch-up samples. Six different samples were created by applying flat interior latex house paint to a 2’ by 2’ panel of standard paper coated gypsum wallboard. Three types of paints (A, B, C) were used, each of them varying in their chemical formulations. Two commonly used application methods were used- airless spraying and rolling.

Initially, a base coat was applied over the whole panel- three panels each using spraying and rolling methods. Once this coat had dried, a 1’ by 1’ region in the center of the panel was “touched-up” with a second coat applied with a fabric roller. Each of the panels was assigned sample numbers to make data gathering easier.

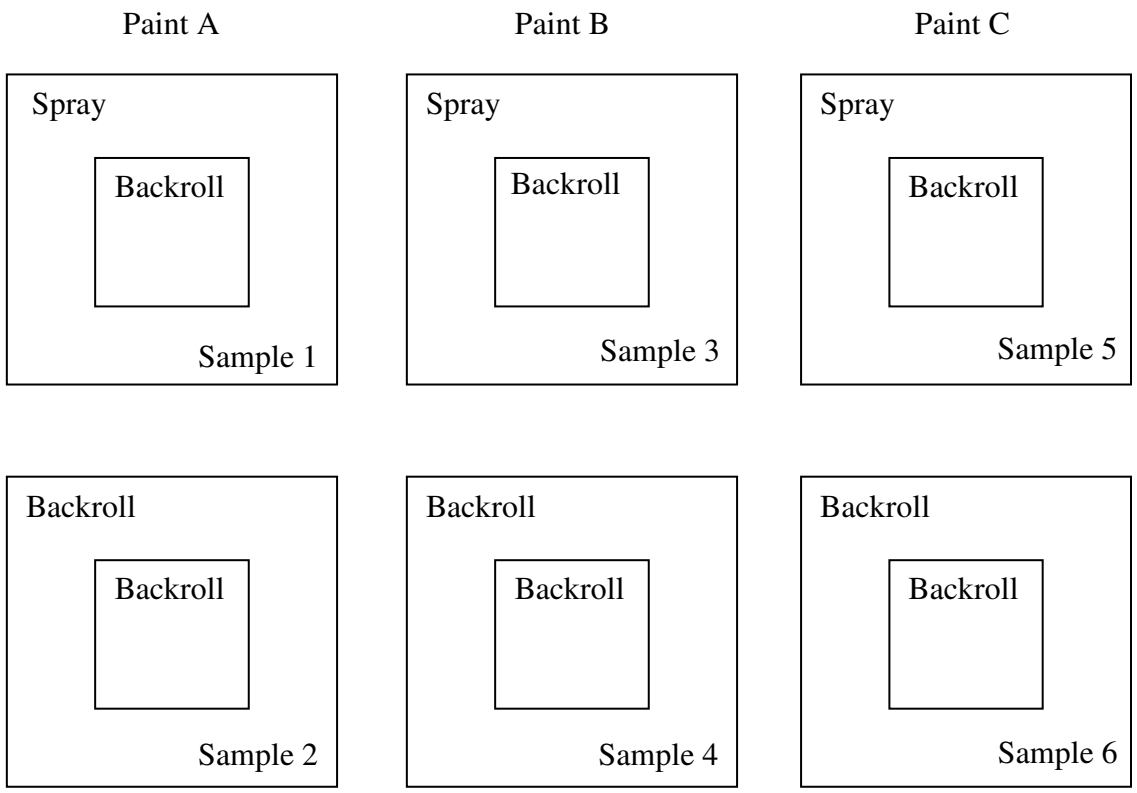

Figure 11: Samples created for the psychophysical experiments and measurement. Each sample was given a number as indicated in the lower right corner, for ease of data recording. Three kinds of paints and two commonly used application methods (spray and roll) were used to prepare the samples.

3.1.1 LIGHT SOURCE SELECTION

Physical inspection of the samples under different lighting and viewing conditions illustrated the touch-up effect. However, in order to obtain measurable results, it was important to be able to document this effect. The easiest way to do this was to attempt to recreate these real-time observations using physical photographs. Various lighting and viewing configurations were used in order to finalize the arrangement that best captures this effect.

In order to explore the effects of light source geometry on the touch-up visibility, the samples were first photographed with a point, linear and area light source. A 5’ by 7’

white LED light box was used and sections of the light box were masked off using cardboard to simulate the different lighting geometries. Samples were photographed with the light source and camera at 60° from the normal.

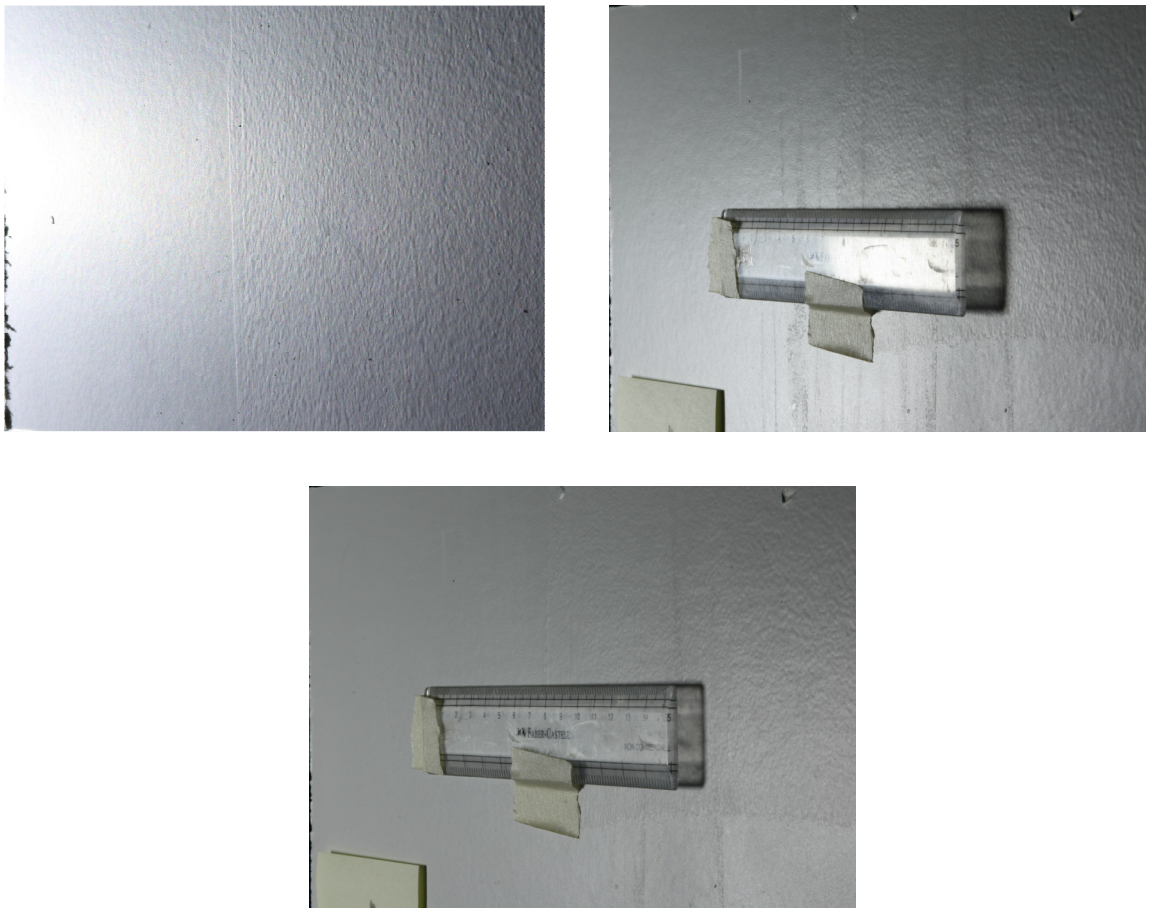

Figure 12: Image capture using different light sources- point (top-left), linear (top-right), and area (bottom)

From these images, it was evident that the area light source was more effective in capturing the differences between the base and touch-up regions, compared to a point or linear light source. In the first two images, there is a very specific “hot-spot” causing uneven illumination across the image. This problem is eliminated with the use of an area light source. Also, the area light source can also be used to simulate lighting from a window or overhead fixture, as would be the case in most natural environments. Hence, it was decided to use an area light source.

3.1.2 SELECTION OF CONFIGURATIONS

To verify that the sample produced a measurable touch-up effect, we photographed it with a Canon EOS XSi 12 Megapixel digital camera. The camera was set to provide good depth of field and good noise response. A 28-105 mm lens was used with the lens completely zoomed in (105 mm). The ISO was set to 100 and aperture was set to F29. The field of view obtained at this setting was 20°. The camera and light source were placed at a distance of 60 cm from the sample. The images were captured in the Canon RAW (CR2) format with an Adobe RGB colorspace.

The samples were photographed at a range of illumination angles from 40° to 80° off the surface normal. The camera was first placed at an angle of 0° (normal to the samples), and then at 60° off the surface normal and opposite to the light source. An analysis of these images helped get an idea of how the touch-up effect manifests itself at different configurations. The purpose of this experiment was to identify the configurations that would represent the best and worst cases of touch-up visibility. Figure 13 shows the series of images produced by focusing on the edge between the sprayed base region (left half of each image) and the rolled touch-up region (right half of each image). The viewing is oblique, at 60° off the surface normal. Each panel shows the appearance at a particular illumination angle. As is observed, there is a visible difference in surface texture and lightness as illumination goes from near normal (40°) through specular (60°) to grazing (80°). The distinct difference in surface lightness and texture can be seen between the two regions, with the base region generally appearing smoother and lighter than the touch-up region.

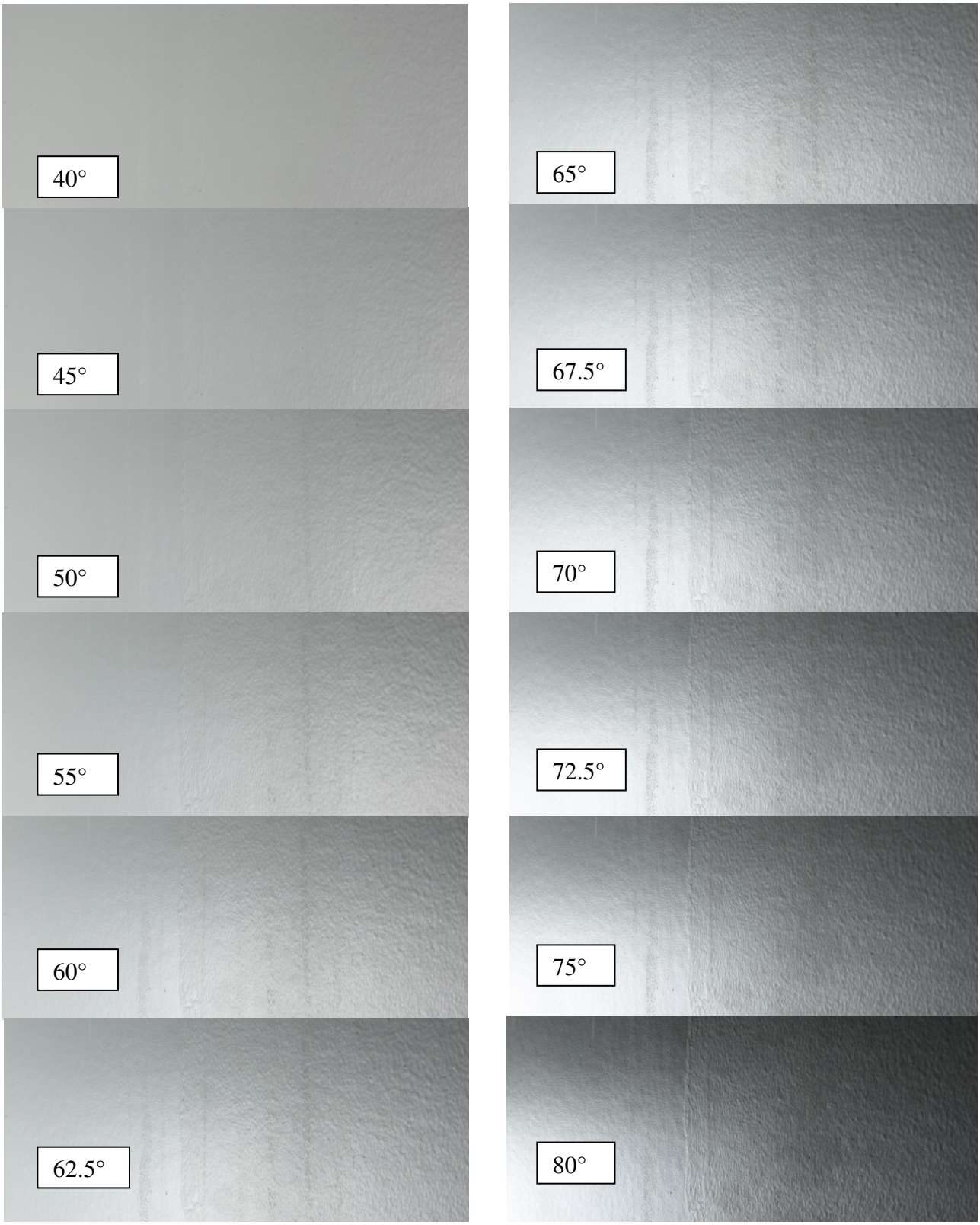

Figure 13: Cropped photographs of the edge between the sprayed base and rolled touch-up regions of a sample.

Observation of the image set showed that the touch-up visibility is most pronounced when the sample is illuminated at 72°. This was identified as the potential "worst-case" scenario. Comparing this with normal viewing and specular lighting revealed that in this configuration, shadowing was an important factor that contributed to appearance differences. To lend symmetry to the experiment, images were also taken at normal lighting and grazing viewing, where lightness differences were more enhanced.

Configuration	Camera Angle	Illumination Angle
1	60°	72°
2	60°	0°
3	0°	72°

Table 2: Different configurations used for taking photographs of the samples

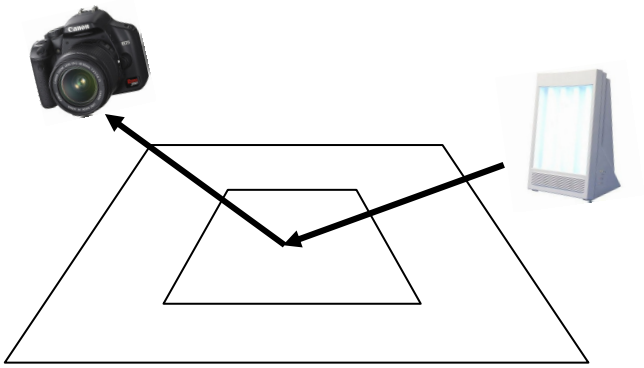

Figure 14: Configuration 1- V60_L72

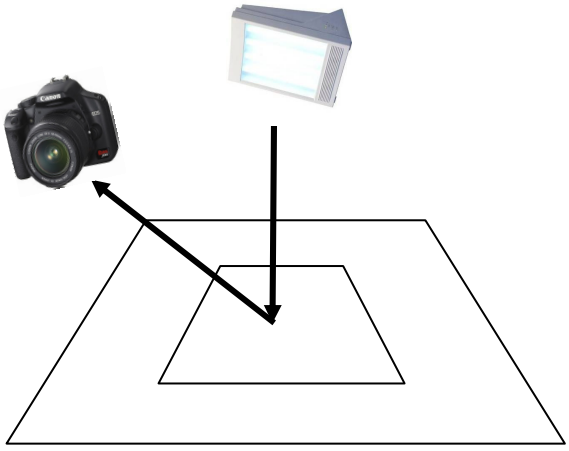

Figure 15: Configuration 2- V60_L0

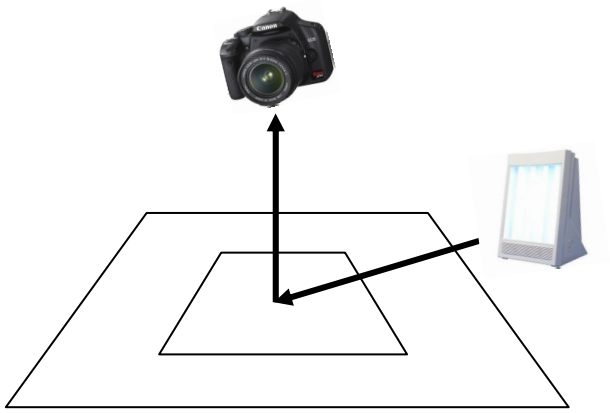

Figure 16: Configuration 3- V0_L72

3.2 DESIGN OF PSYCHOPHYSICAL EXPERIMENTS

The aim of the psychophysical experiments was to determine the smallest perceptible difference (or just noticeable difference) in touch-up visibility. Hence, it was decided to use a Two-Alternative Forced Choice (2AFC) procedure for the experiments. In this design, pairs of stimuli are shown to the subject and they are forced to make a choice between them, even if they cannot detect a difference. Two experiments were designed, each with specific objectives in mind. The purpose and experimental design is described below.

3.2.1 EXPERIMENT 1

The purpose of the first experiment was to determine the effects of four variables- paint formulation, application methods and lighting and viewing conditions on touch-up visibility. Hence, the main experimental design consisted of images that captured a wide range of touch-up differences. The following conditions were used:

(i) Types of Paints- A, B, C
(ii) Types of Application Methods- Spray and Roll
(iii) Types of Viewing/Lighting combinations- V60_L72, V0_L72, V60_L0

Hence, the total number of stimulus images = 3 paints x 2 application methods x 3 configurations = 18 images

Number of trials = 18 x (18-1)/2 = 153 trials

3.2.2 EXPERIMENT 2

Experiment 1 will help establish the visibility of the touch-up region as a function of the paint formulation, application method, lighting and viewing condition. The purpose of the second psychophysical experiment is to study whether the edge has an effect on the human perception of a difference in appearance between the two regions. There was a possibility that the distinct edge present between the base and touch-up replicated a Craik-O'Brien-Cornsweet illusion when viewed by an observer.

The Craik-O'Brien-Cornsweet effect is a visual illusion where luminance of enclosed boundaries sets the brightness of the enclosed regions (Cornsweet, 1970). For example, consider Figure 17 below. The region to the right of the edge appears slightly lighter than the region to the left of the edge. But if the central region is blackened out, thus "removing" the edge, it can be seen that the two areas in fact have the exact same brightness. Figure 18 shows the difference between the actual distributions of luminance in the image versus the perceived distribution.

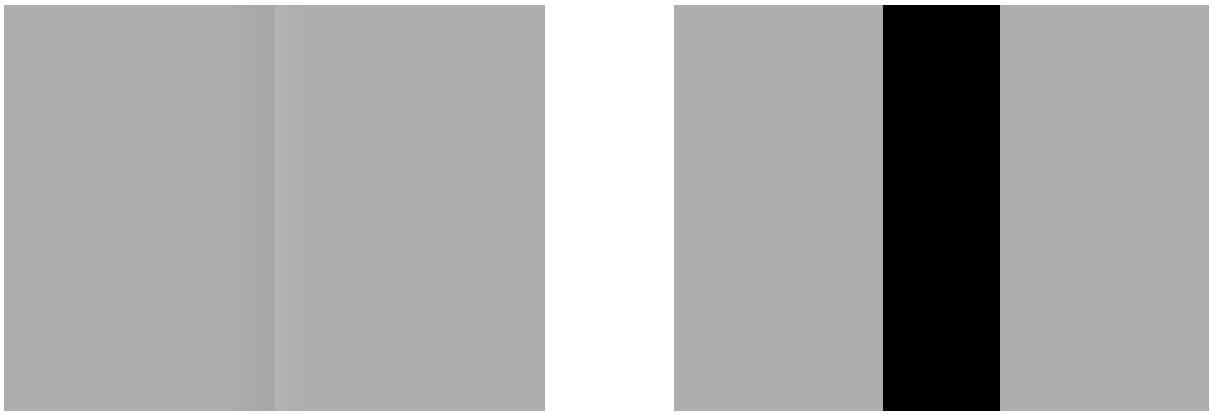

Figure 17: The Cornsweet illusion- In the image to the left, the left part of the picture seems to be darker than the right one. They, in fact, have the same brightness. In the right image, the edge in the middle is hidden. This makes the two sides seem like they have the same color.

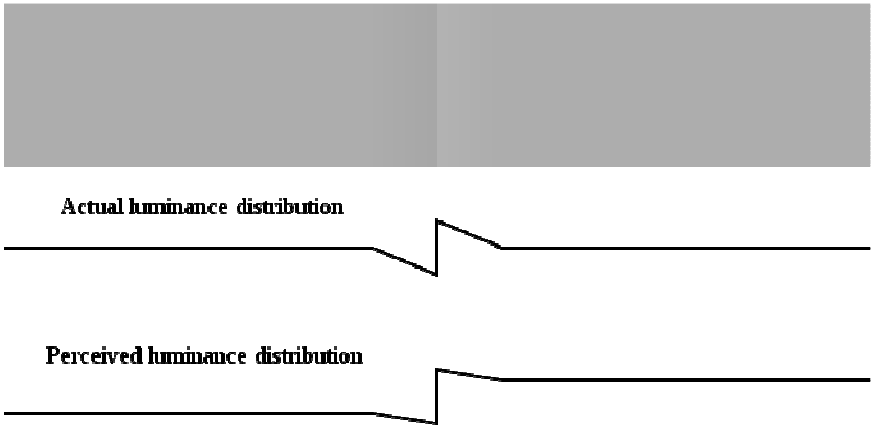

Figure 18: The actual distribution of luminance in the image above, and the perceived distribution of luminance.

For this experiment, it was necessary to physically create different "types of edges", in order to judge the effect of the contours on the touch-up visibility. Only the images from the worst case scenario (V60_L72) were used in this experiment. In order to estimate the placement of the edge samples above or below the threshold based on the natural variance in the spray and rolled sides, the images of *only the base regions* of paint C were also included in the study. These were called "Null" images. The reason for including only paint C is that it has the least visible differences between the base and touch-up regions. Hence, the following conditions were used:

(i) Types of Paints: A, B, C

(ii) Types of Application Methods: Spray and Roll

(iii) Types of Lighting/Viewing Combinations: V60_L72

(iv) Types of Edges (described in detail on Page 40): Normal, Sharp, Blend + 2 Nulls

Hence, number of stimulus images = 3 paints x 2 application methods x 1 lighting/viewing condition x 3 edges + 2 nulls = 20 images

Number of trials = 20 x (20-1)/2 = 190 trials

3.3 STIMULUS PREPARATION

As mentioned earlier, the images captured using the digital camera was in the Canon RAW (CR2) format. They needed to be processed to make the stimuli suitable for each of the experiments. The detailed procedure used for processing the stimuli for each experiment is described below.

3.3.1 EXPERIMENT 1

The CR2 images that were captured using the camera could not be used as-is for the experiments. The field of view was 20° with the focus set to the edge between the base and touch-up. Hence region outside the FOV needed to be cropped out. Secondly, since the sample was illuminated at an angle, the luminance across the horizontal plane of the image was not equally distributed. These modifications needed to be made in order to process the images for the experiments. The following steps were performed:

(i) Central 1200x600 pixel sections were cropped from the original 4272x2848 pixel images such that the edge is approximately centered in the image.

(ii) The embedded color profile was discarded and the G-channel was converted to grayscale

(iii) A high-pass filter was applied to equalize luminance across the image

These images were termed the “normal” set of images for the six samples.

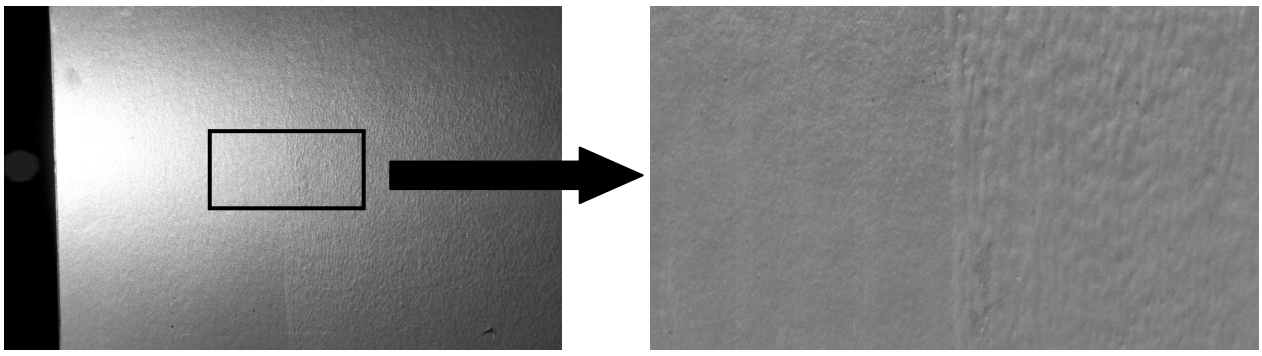

Figure 19: Stimulus preparation for Experiment 1. The image to the right is for paint A, with a sprayed base, at configuration V60_L72

3.3.2 EXPERIMENT 2

The initial processing was the same as described to create the "normal" image set for Experiment 1. Following this, the following types of edges were created using Photoshop.

(i) Normal edge: The original edges on the samples were used as-is, without any modifications

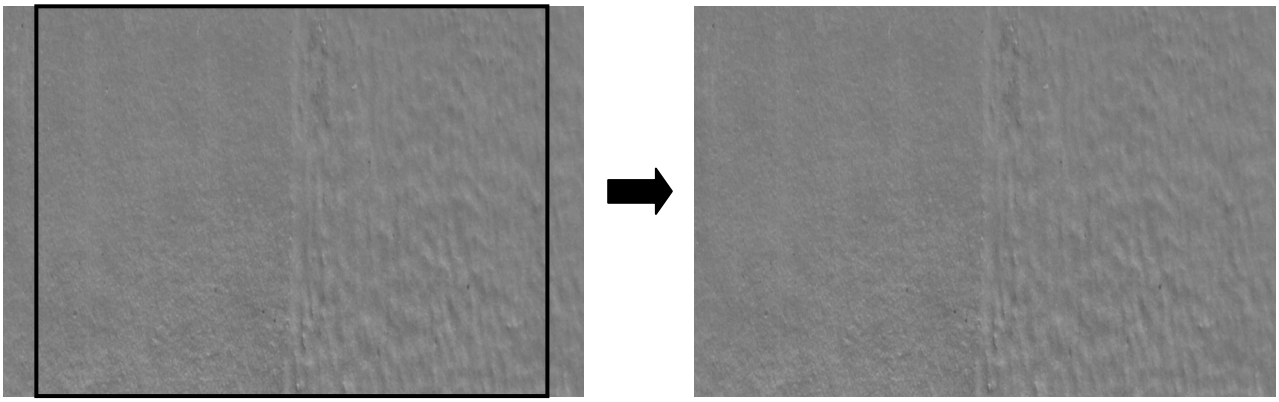

Figure 20: Stimulus preparation for Experiment 2. The image to the right represents the normal edge stimulus for Sample 1 at V60_L72 configuration

(ii) Sharp edge: Sections of the base and touch-up regions excluding the edge were cropped and placed side by side to create a sharp, straight-line edge.

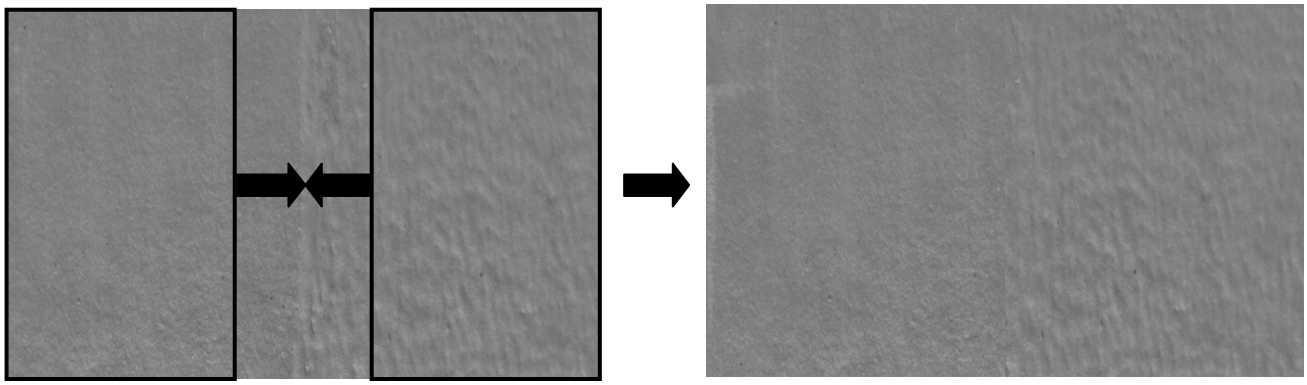

Figure 21: Stimulus preparation for Experiment 2. The image to the right represents the sharp edge stimulus for Sample 1 at V60_L72 configuration

(iii) Blend edge: The transparency of the edge in the sharp images was modified so that it appears to blend in with the surrounding base and touch-up

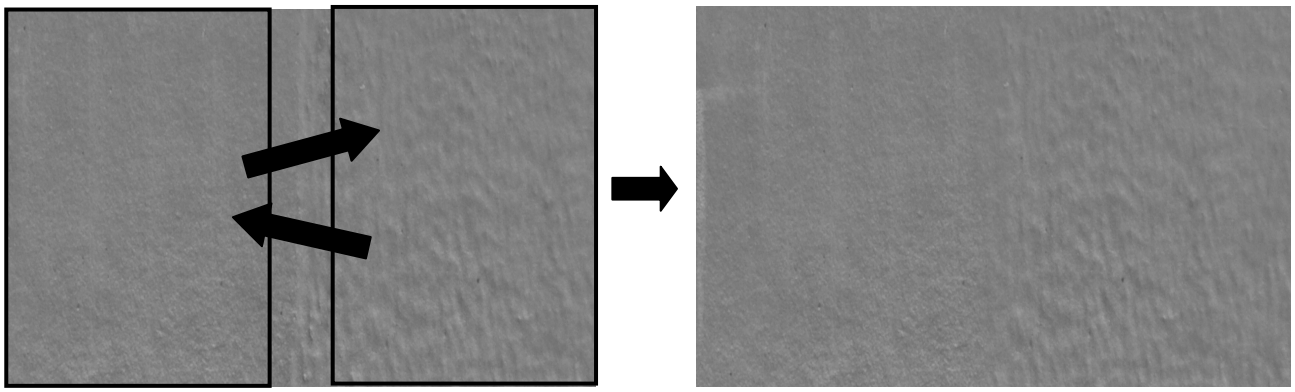

Figure 22: Stimulus preparation for Experiment 2. The image to the right represents the blend edge stimulus for Sample 1 at V60_L72 configuration

(iv) Null sample: A 1200x600 crop-out of just the base region for sample with paint C was used to create the null images.

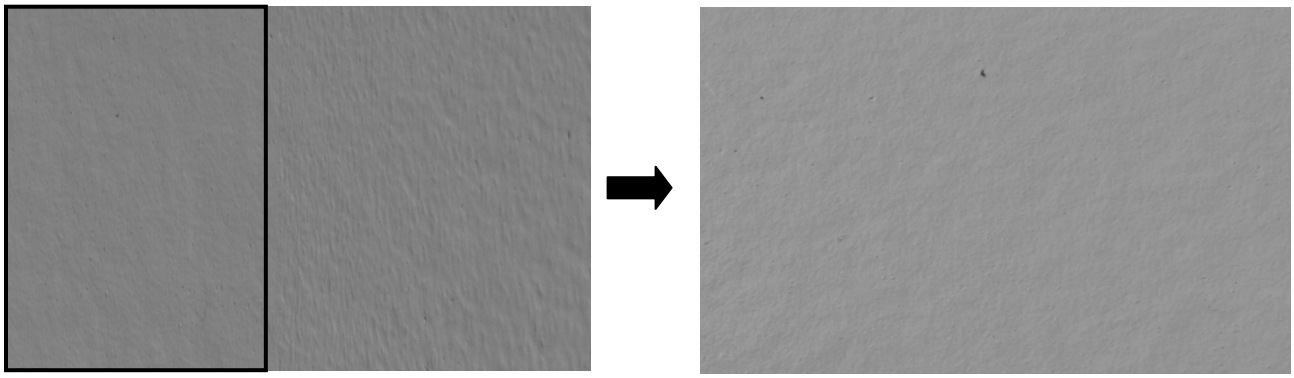

Figure 23: Stimulus preparation for Experiment 2. The image to the right represents the null stimulus for Sample 5 at V60_L72 configuration

3.4 EXPERIMENTAL PROCEDURE

30 subjects, ages 20 to 40, participated in each experiment. They were all naïve to the methods of the experiment. All had normal or corrected to normal vision.

In the experimental session, the subjects viewed pairs of images displayed on a calibrated 30-inch Apple Cinema display. The monitor resolution was set to 2560x1600 and the system gamma was 2.2. The images were presented on a black background in a darkened room. Given the standard resolution of the display (100 dpi) and the field of view of the camera, it was found that the display has a magnification of 3 with respect to the viewing distance. The original images were captured with the camera at a distance of 24 inches from the sample. This means that when displayed on the monitor, it would be equivalent to viewing them from a distance of 8 inches. Therefore, in order to retain the effect of the original viewing distance of 24 inches, the subjects were made to view the monitor from a distance of 72 inches (or 6 feet). At this viewing distance, each image subtended 2 degrees of visual angle. Figure 24 demonstrates the set-up of the experiment.

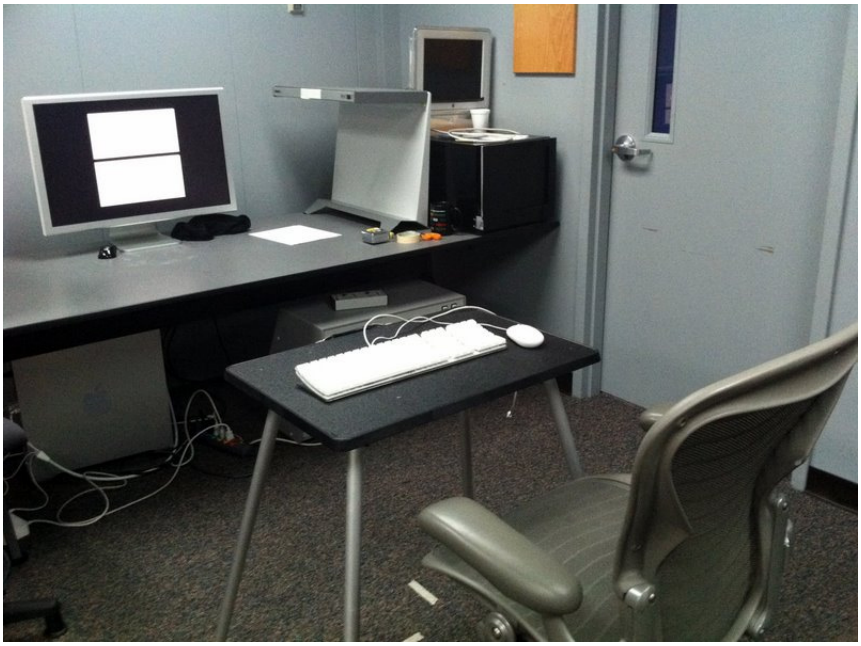

Figure 24: Set-up for the psychophysical experiments. Participants were asked to view the screen from a distance of 6 feet. The experiments were conducted in a dark room.

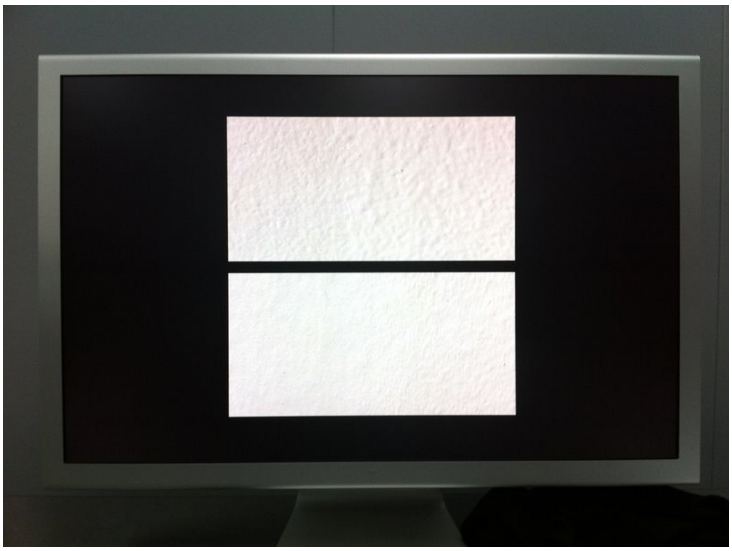

Figure 25: Stimuli were displayed on a 30-inch Apple Cinema display in a top-bottom arrangement.

The exact set of instructions was given to each subject. They were told that images would be presented in top/bottom pairs and were asked to choose the image that had a greater difference in appearance between the left and right sides. They were told to neglect dust specs and blemishes that might be a part of certain digital images and instead, focus on the overall appearance of the images on the screen. They entered their responses by pressing the up/down arrows on the keyboard. All the image pairs were presented in a completely randomized order. For each subject, the results were recorded in the form of a 153x3 matrix where the first two columns represented the top and bottom images displayed and the last column recorded the choice made by the subject.

3.5 RESULTS

Using Thurstone's Law of Comparative Judgments (Thurstone, 1927), the preferred selections from the observers were transformed into a frequency matrix that recorded the numbers of selections for each image. After that, a proportion matrix was transformed through dividing the frequencies by the total number of observations. Finally, the proportions were converted into Z-scores and the interval scales were obtained by

averaging each column of the Z-scores. This method helped derive a relative touch-up visibility scale.

3.5.1 EXPERIMENT 1

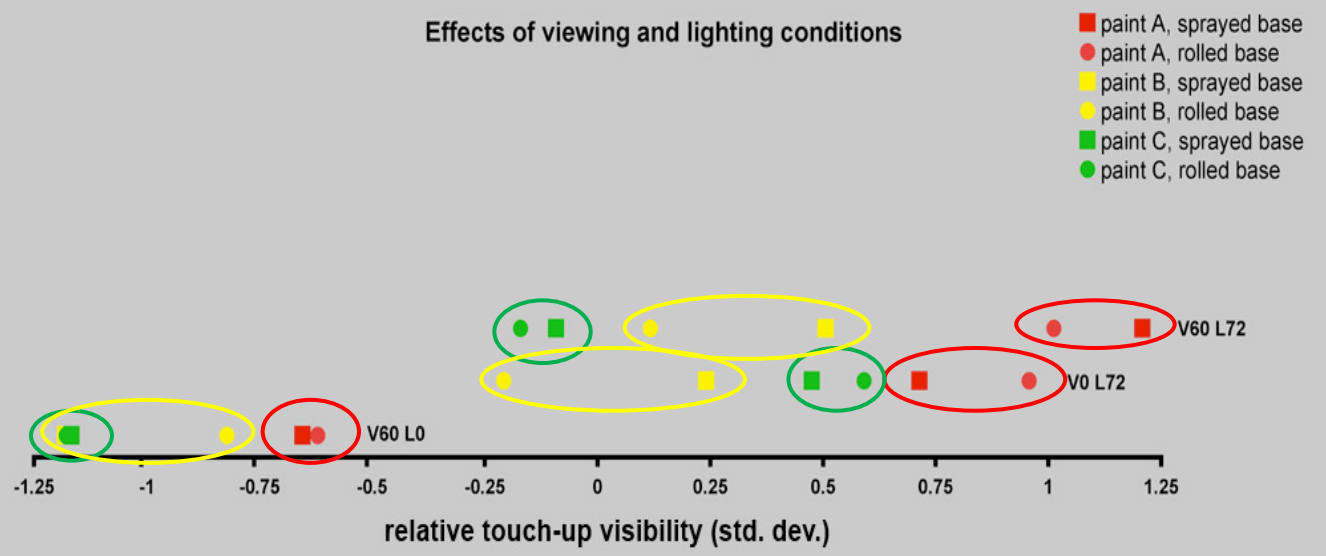

Figure 26: Results obtained from Experiment 1

In the Thurstonian scale shown in Figure 26, the horizontal dimension represents the different lighting and viewing conditions. Each type of paint is represented by a different color, as mentioned in the key in the top right corner. Also, each application method is indicated by a different shape- the square dots represent a sprayed base and rolled touch-up, whereas the round dots represent a rolled base and rolled touch-up. Note that the scale represents a standard distribution of the results and hence, the points in the central region represent the conditions where observed differences between the base and touch-up region are minimum.

If the three configurations (V60_L0, V0_L72 and V60_L72) are compared, it is seen that within each of these sets, the touch-up visibility is affected by the paint formulation and paint application method. Generally speaking, samples created using paint A show the maximum difference between base and touch-up. Also, in most of the samples the sprayed base and rolled touch-up show a greater difference in appearance than a rolled

base and rolled touch-up. Both of these conclusions are intuitive, based on physical observation of the samples. Another conclusion that can be drawn is that the difference in visual appearance between the sprayed base and rolled base for samples created using Paint B is a lot greater than for Paints A and C. This is evident from the larger distance between the yellow dots (representing Paint B) on the graph, compared to the red and green dots for each configuration.

If the lighting and viewing conditions are now compared, it can be seen that there are some improvements in the touch-up visibility with viewing conditions (from specular viewing (V60) to normal viewing (V0)). However, there are dramatic improvements with lighting conditions (from grazing illumination (L72) to normal illumination (L0)). The final visibility of the touch-up region is a combination of the interaction of these four factors. Lighting and viewing conditions cannot always be controlled since they largely depend on the environment and personal choice. Hence, if touch-up visibility is to be controlled, it is more beneficial to focus on the paint formulation and application methods in order to minimize the touch-up problem.

3.5.2 EXPERIMENT 2

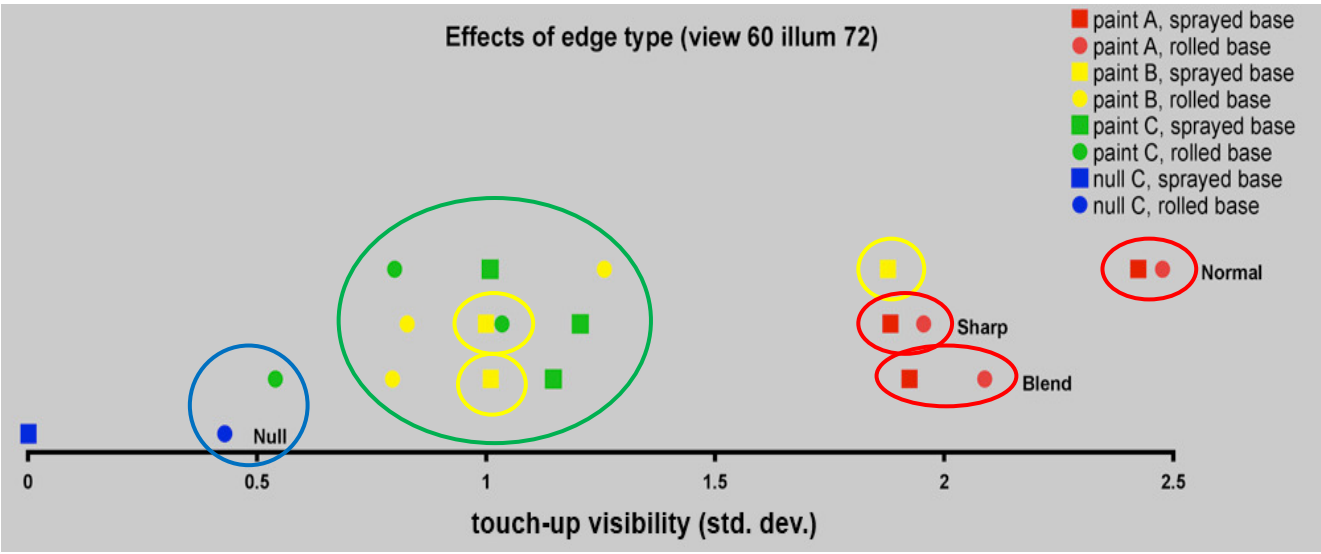

Figure 27: Results obtained from Experiment 2

In the scale shown in Figure 27, the horizontal dimension represents the different types of edges. Each type of paint is represented using a different color. Note that the null samples of Paint C are considered as a different category from the regular touched-up paint C samples. As in the case of the first scale, square dots indicate a sprayed base and rolled touch-up, whereas round dots indicate a rolled base and rolled touch-up. In order to obtain a comparison between the different types of edges, the sprayed null sample was affixed at zero standard deviation and the other points were scaled appropriately. Hence, on this scale, as one moves to the right, the points represent increasing difference between base and touch-up regions, as judged by the subjects.

Firstly, if the three types of edges are compared for paint C (green dots), it can be seen that the samples with a sprayed base (green square dots) fall in the same range of standard deviation compared to the rolled base (green round dots). This means that the sprayed base shows a more similar behavior in terms of perceptual appearance regardless of the type of edge on the sample. Overall, it can be seen that the behavior of the edge varies with the type of paint.

If we compare the effect of the type of edge for each type of paint, it is evident that the edge affects the magnitude of touch-up visibility for paints A and B more than for paint C. For both these paints, there is an improvement in touch-up visibility when the edge is sharp or blended instead of normal. However, for paint C, the type of edge does not necessarily govern the end result. Specifically in the case of samples that have been sprayed using paint B (yellow square dots), there is a significant improvement in the perceptual appearance of the sample when a normal edge is modified to a sharp or blended edge.

The two null samples can be considered to be ideal conditions with nearly zero touch-up visibility. Comparing the other conditions with these ideal samples, it can be inferred that a blended edge with a rolled base and rolled touch-up, applied using paint C is the “near-ideal” scenario. Hence, it follows that one of the techniques of minimizing the touch-up visibility is by using a good paint with similar application methods and well-blended regions.

3.6 DISCUSSION

The scales developed above give a good qualitative analysis of the factors that govern the touch-up problem. From all the independent variables in the experiments, it can be concluded that paint formulation, application methods and edge properties are the most significant factors that affect this problem. Lighting and viewing conditions play a significant role in the enhancement or reduction in the perceptual magnitude of this effect. However, these conditions cannot be controlled in all commercial situations. At the same time, the physical conditions such as the formulation and application methods are within actual manipulation. If an attempt is made to relate these physical characteristics with the surface properties of the painted surface, then concrete measures can be taken to solve this problem.

Figure 28 shows a touched-up region where the base is sprayed and a rolled touch-up coat is applied on it.

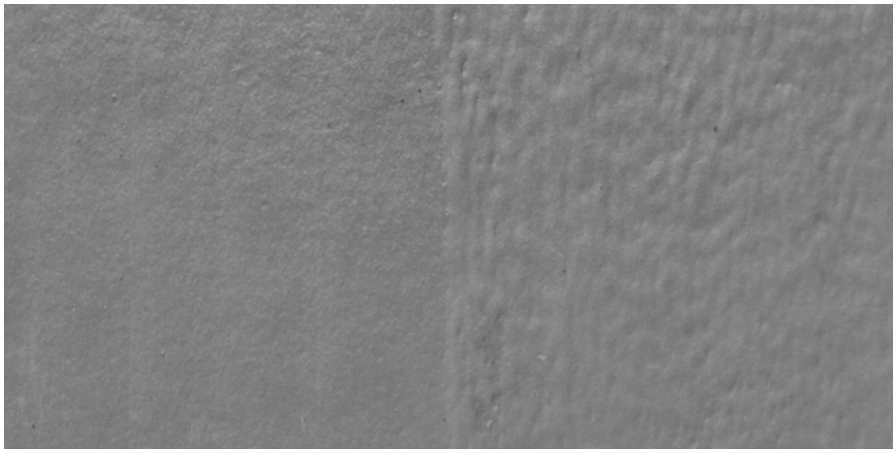

Figure 28: Image of Sample 1- with sprayed base and rolled touch-up. The image is taken at a specular viewing and off-specular illumination angle.

Visual examination of this surface reveals that there are differences in both the reflectance and textural properties of the base and touch-up region. In qualitative terms, the touch-up region appears lighter and rougher than the base, thus leading to a significant difference in

the appearance of these two regions. Correlating this difference in visual appearance to difference in physical surface properties can help determine the physical causes for the touch-up problem and thus can enable designing of techniques to help solve it. Hence, the next part of the project deals with the physical measurement of these surface properties. As described earlier, different surface properties are manifested at the microscale and mesoscale level. At the microscale, the BRDF is used to describe the way a surface scatters light. At the mesoscale level, difference in surface texture causes difference in appearance.

4 SURFACE MEASUREMENT

4.1 REFLECTANCE MEASUREMENTS

At the microscale level, surface reflectance can be described using the bi-directional reflectance distribution function (BRDF) that characterizes how the surface scatters incident light. BRDF measurements of the base and touch-up regions of the samples were done using a Murakami GSP-1B gonio-spectrophotometer in the Munsell Color Science Laboratory. The construction of this instrument is described in section 4.1.1.

4.1.1 THE GONIO-SPECTROPHOTOMETER

A gonio-spectrophotometer is a device designed for measuring gonio-apparent materials, that is, materials that change in appearance because of difference in viewing and illumination angles. This device measures the spatial distribution of reflected light at various combinations of illumination and detection angles selected by the user. The measurement of the spectral distribution of every pair of illumination and detection angles is performed individually, based on the precise control of incident and acceptance angle. The data measured by this instrument is used for the development of gonio-apparent material matching as also for graphics rendering models.

Figure 29 below shows the GSP-1B Gonio-spectrophotometer that is available in the Munsell Color Science Laboratory.

Figure 29: GSP-1B Gonio-spectrophotometer (AvianGroupUSA, 2009)

Figure 30 on the next page shows the inside view of the gonio-spectrophotometer. The sample (5) is clamped onto the sample stage which has a manually-adjustable tilt angle, also called the “flop”. The reference white plate (6) is barium-sulfate coated and is placed onto the second stage below the sample. It remains in the same position throughout the measurement process. The sample platform (2) rotated according to the parameter setting made in the software between the limits of -80° and +80° perpendicular to the sample plane.

The lamp housing (1) has a single tungsten halogen source lamp. This is divided into two identical beams- the sample beam (1S) and reference beam (1R) via mirrors, lenses and heat filters. The lamp housing rotates on the same axis as the sample platform so that the incident angle can be varied.

The two light beams exit through the apertures and fall on the sample and reference plate which reflect them back to the sample receptor (7S) and reference receptor (7R) respectively. Each beam is directed to the fixed detection system via a mirror and beam chopper assembly. This assembly, in turn, directs the beams to the monochromator via a lens system. The light from the monochromator is dispersed into each wavelength via a diffraction grating and this is converted to the elements of a photodiode array. The electrical signals are then amplified, transformed into digital signals using an A/D converter and then transmitted to the PC via a GP-IB IEEE interface for processing into the user-selected color scales and displays.

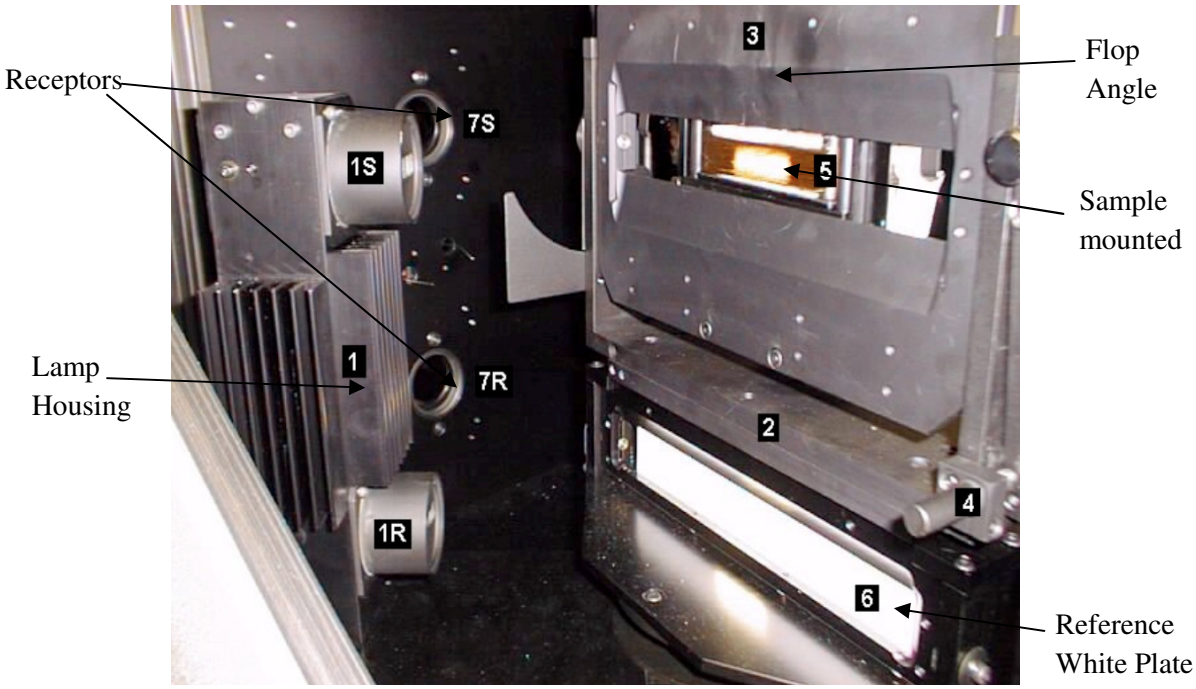

Figure 30: Interior of the GSP-1B Gonio-spectrophotometer (AvianGroupUSA, 2009)

Table 3 shows the specifications of the instrument: (Source: (AvianGroupUSA, 2009)

Measuring System	Dual-beam optics with Reference Plate
Measuring Geometry	Adjustable illumination and viewing angle
Light source	12V 100W Halogen Lamp
Lamp Life	1000 hours nominal
Dispersing element	Concave diffraction grating
Detector	Silicon photodiode array
Wavelength range	390 – 730 nm
Wavelength interval	10 nm
Spectral Bandpass	Approx 10 nm
Wavelength accuracy	± 1 nm @ 560 nm
Wavelength repeatability	± 0.1 nm
Incident angle range	±80°
Receiving angle range	±80°
Angular accuracy	Within ± 0.5°
Angular resolution	0.1° (of absolute encoder)
Viewed area	Approx. 8 x 16 mm at 0° receiving angle Approx. 8 x 94 mm at 80° receiving angle
Source Aperture Angle	± 1.05° in plane of measurement ± 2.10° perpendicular to plane of measurement
Receptor Aperture	± 1° in circle
Neutral Density Filter Range	Reduces sample to 30, 10, 3, 1, 0.3, 0.1 or 0.03%
Measurement Duration	Approx. 3 seconds per angle increment
Measurement Accuracy	Within ±0.5%

Repeatability	0.05% SD
Dimensions (mm)	566 (W) x 972 (D) x 922 (H)
Weight	86 kg
Power Requirements	100V AC, 50/60 Hz, 4A
Computer Interface	GP-IB (PC) F by Contec Ltd

Table 3: Specifications of the Murakami GSP-1B gonio-spectrophotometer

4.1.2 BRDF MEASUREMENTS

In-plane measurements with source angles at 15, 30, 45 and 60 degrees were taken. The setup for reflectance measurements and the results obtained are shown in figures 31 and 32 respectively.

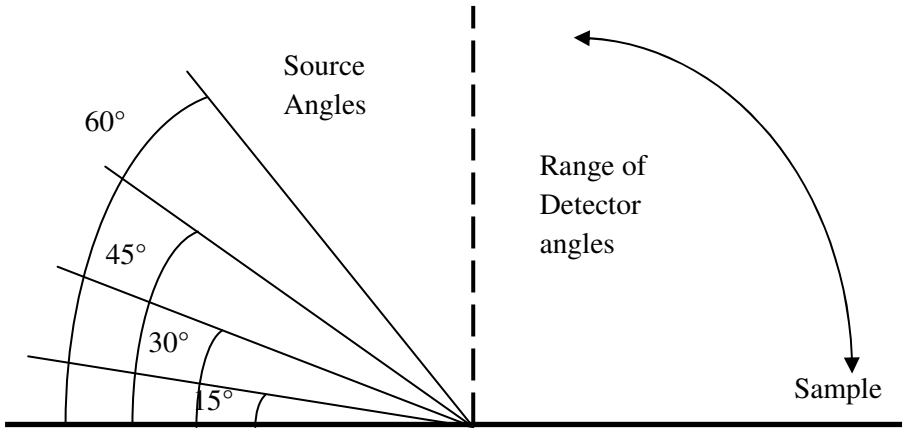

Figure 31: Set-up for reflectance measurements using the Murakami gonio-spectrophotometer

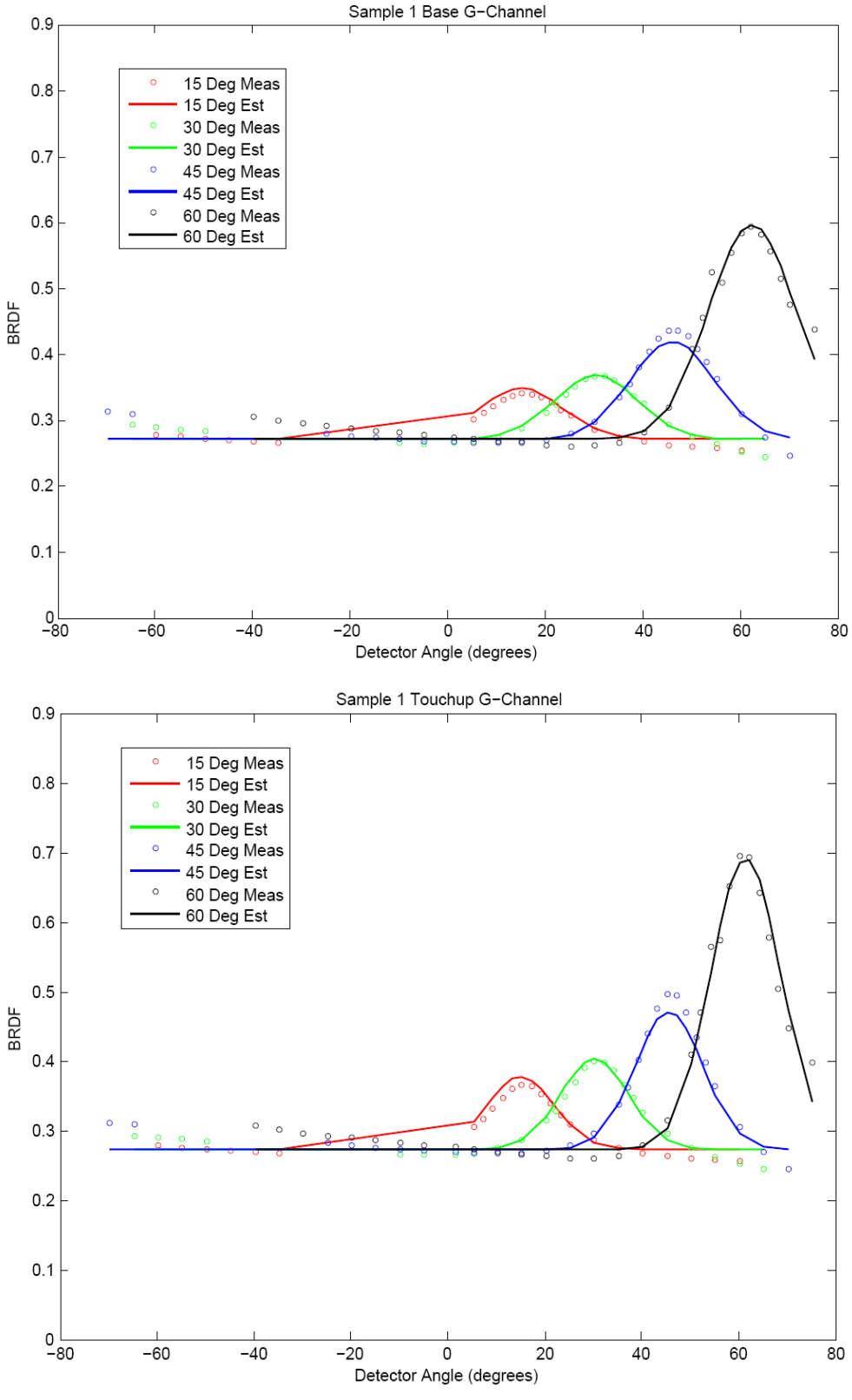

Figure 32: BRDF measurements for sprayed base (top), and rolled touch-up (bottom)

In Figure 32, the open circles show the data for the base region. As is seen in this graph, the magnitude of the specular reflection (when detector angle equals source angle) increases with source angle. This is due to the Fresnel effects that cause an otherwise matte surface to appear glossy with viewed at grazing angles. The wide spreads of the distributions indicate that even at grazing angles (60° and higher), the surface has relatively low gloss.

The lower graph shows the data for the touch-up region. The behavior is similar in both the graphs with respect to change in source angle. However, for the touch-up region, the distributions are higher and narrower than those of the base region.

This indicates that over the range of spatial scales measured by the gonio-spectrophotometer, the *touch-up region is optically smoother than the base region*. These reflectance (gloss) differences make the touch-up region looks lighter than the base under oblique illumination and viewing conditions.

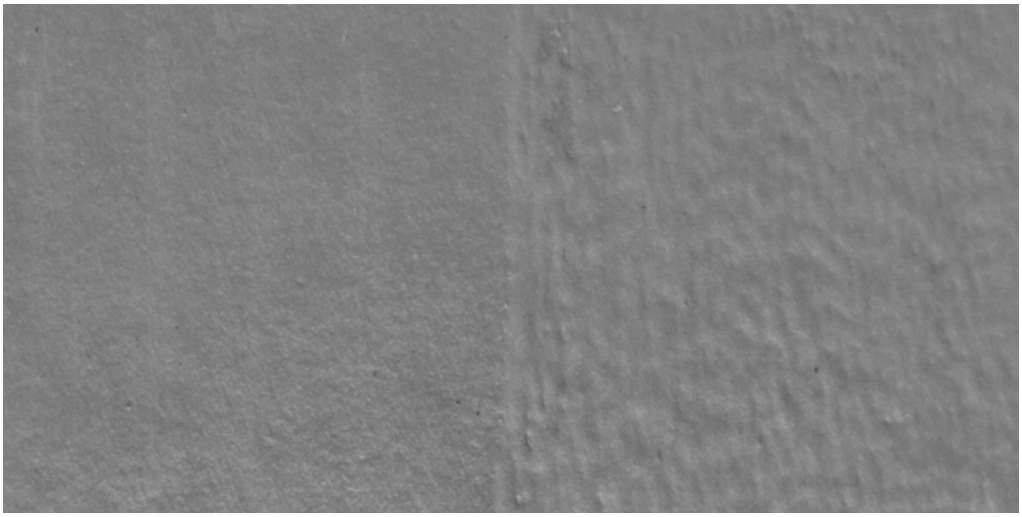

Figure 33: Image of Sample 1- with sprayed base and rolled touch-up. The image is taken at a specular viewing and off-specular illumination angle.

4.2 TOPOGRAPHIC MEASUREMENTS

In addition to its reflectance properties, significant information about the visual appearance of a surface can be derived from its topographical features. Measurement of the mesoscale textures of the base and touch-up regions of the sample was performed using photometric stereo to derive surface normal maps.

The experimental setup is illustrated Figure 34. The paint sample is placed on a flat test bed. A camera is placed directly over the sample. A regular fluorescent tube is used as the light source, mounted on a rotating arm. The sample is first illuminated from the left hand side and an image of the sample is captured. Next, the same light source is moved to the right hand side and another image is captured. This process is repeated separately for the base and touch-up regions of the sample. The angle of illumination (α) was maintained at 32° from the horizontal plane. The camera field of view was 36.8mm. The resolution of the images captured by the camera was 640 x 480 pixels. Therefore the scaling obtained was approximately 0.07mm/pixel.

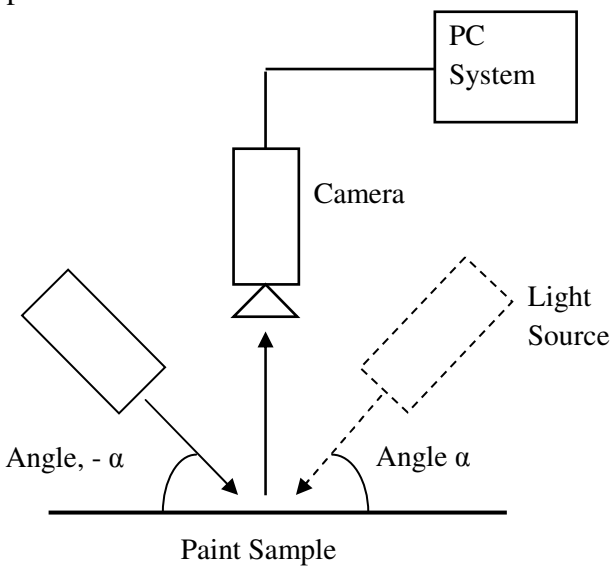

Figure 34: Experimental set-up for photometric stereo method

The raw images obtained by illuminating the sample 1 from the left and right sides are shown below. In order to compensate for the uneven illumination across the image, a flat field correction was applied to each of them.

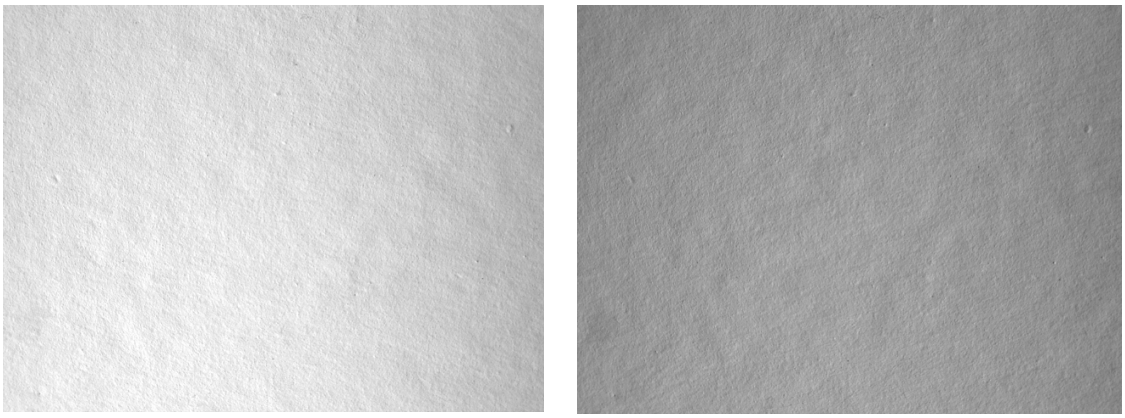

Figure 35a: Raw images of the base area for Sample 1, with sprayed base coat and rolled touch-up. The left image was captured when the base is illuminated from the left side and the right image shows the base area illuminated from the right side.

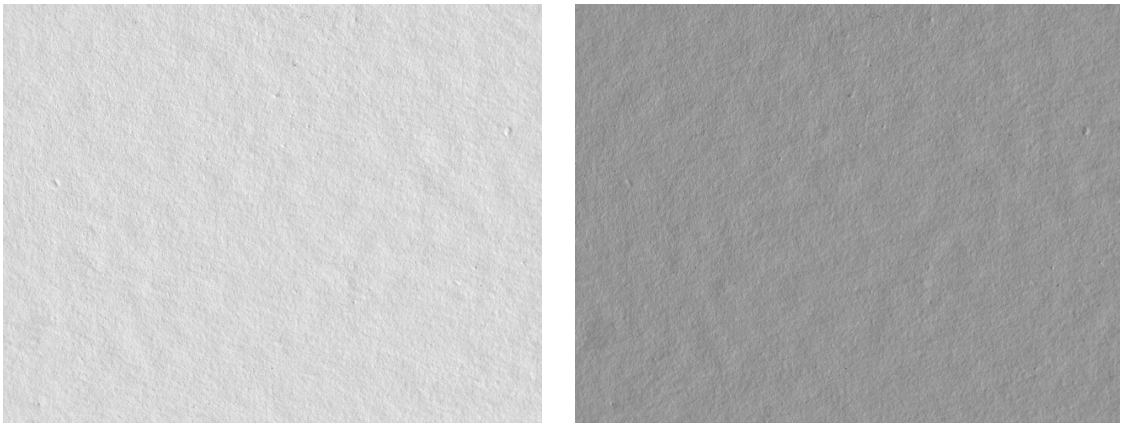

Figure 35b: The same images after flat field correction

Representative images showing the texture differences between the base and touch-up regions are shown in Figure 36.

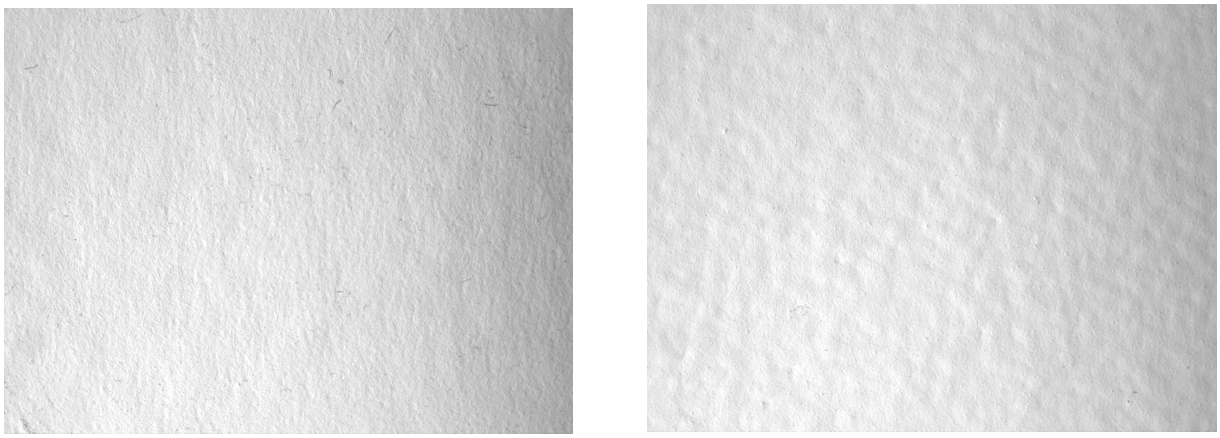

Figure 36: Images of Sample 1 obtained as a part of the photometric stereo method. The left image represents the sprayed base coat and the right image shows the rolled touch-up coat.

These images were then used as input for a noise power analysis of the frequency distribution of the normal angles, in order to characterize the scales of the texture elements on the surface. The MathCAD code used for performing this analysis is reproduced below-

$MT \equiv READBMP("LeftT.tif")$ $FOV \equiv 36.8$

$MB \equiv READBMP("LeftB.tif")$

$Nr \equiv rows(MT)$ $Nc \equiv cols(MT)$

$i \equiv 0..Nr - 1$ $j \equiv 0..Nc - 1$

$x_j \equiv \frac{j}{Nc - 1} \cdot FOV$ $\xi_j \equiv \frac{j}{FOV}$

$ST1_j \equiv mean\left(MT^{\langle j \rangle}\right)$ $SB1_j \equiv mean\left(MB^{\langle j \rangle}\right)$

$ST2 \equiv ksmooth\left(x, ST1, \frac{Nc}{1000}\right)$ $SB2 \equiv ksmooth\left(x, SB1, \frac{Nc}{1000}\right)$

$ST \equiv \overrightarrow{(ST1 - ST2)}$ $SB \equiv \overrightarrow{(SB1 - SB2)}$

$MeanST \equiv mean(ST)$ $MeanSB \equiv mean(SB)$

$st \equiv \overrightarrow{(ST - MeanST)}$ $sb \equiv \overrightarrow{(SB - MeanSB)}$

$FT \equiv cfft(st)$ $FB \equiv cfft(sb)$

$WT \equiv \overrightarrow{\left(Re(FT)^2 + Im(FT)^2\right)}$ $WB \equiv \overrightarrow{\left(Re(FB)^2 + Im(FB)^2\right)}$

$$jj \equiv 0..\,floor\left(\frac{Nc}{22}\right)$$

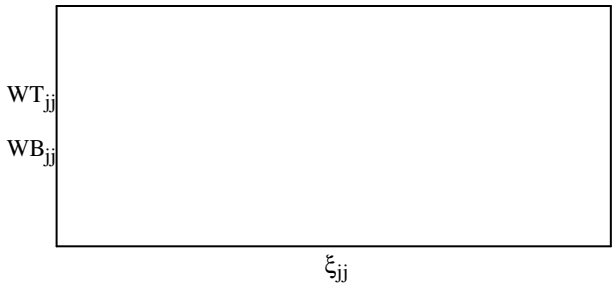

$Spec_{jj,0} \equiv \xi_{jj}$ $Spec_{jj,1} \equiv WB_{jj}$ $Spec_{jj,2} \equiv WT_{jj}$

$WxRITEPRN("Spec.dat") \equiv Spec$ (This saves the two spectra)

$$CWT_{jj} \equiv \sum_{q=0}^{jj} WT_q \qquad CWB_{jj} \equiv \sum_{q=0}^{jj} WB_q$$

$MaxCWT \equiv max(CWT)$ $MaxCWB \equiv max(CWB)$

$$CNWT_{jj} \equiv \frac{CWT_{jj}}{MaxCWT} \qquad CNWB_{jj} \equiv \frac{CWB_{jj}}{MaxCWB}$$

The output of the noise power analysis is obtained in the form of a graph of the noise power of the base and touch-up regions (WB_{jj} and WT_{jj} respectively) versus the spatial frequency of the elements (ξ_{jj}) in cycles/mm. The graphs in Figure 37 represent the noise power spectra for a sample with sprayed base coat and rolled touch-up.

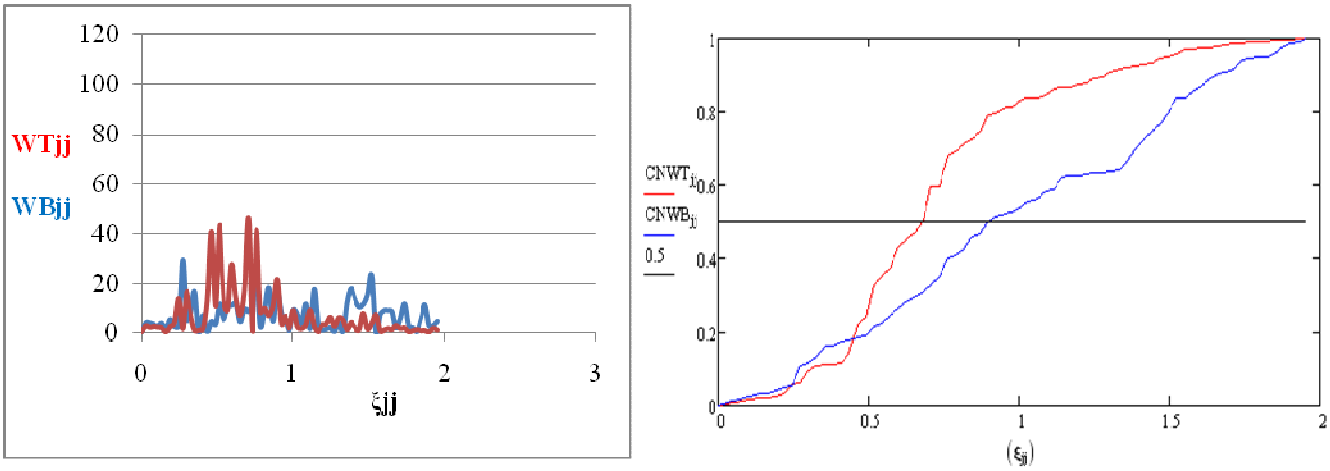

Figure 37: The graph on the left is of the noise power spectra of the base (WB, blue) and the touch-up (WT, red) regions. Note that the spectrum for the touch-up region is concentrated at lower spatial frequencies. The graph on the right is of the cumulative noise power spectra for the base and touch-up.

A comparison of the two regions shows that the base region has a more even distribution over a wide range of frequencies than the touch-up region, which has more energy over a band of lower frequencies. The same phenomenon is reflected in the cumulative noise power spectra ($CNWB_{jj}$ and $CNWT_{jj}$) for the base and touch-up regions respectively. The spectrum for the base is approximately linear while the touch-up region has relatively more energy at lower frequencies. These measured texture differences (along with the previously reported reflectance differences) help explain the appearance changes seen during observation. At the microscale, the rolled touchup region is smoother (glossier) than the sprayed base, causing the observed lightness differences at grazing. At the same time, at the mesoscale, the touch-up region is rougher than the base, causing the observed texture differences.

The same analysis was repeated for a sample with a rolled base and touch-up coat. The images in Figure 38 show the texture differences between the base and touch-up as captured during experimentation and the corresponding graphs of the noise power spectra are shown in Figure 39.

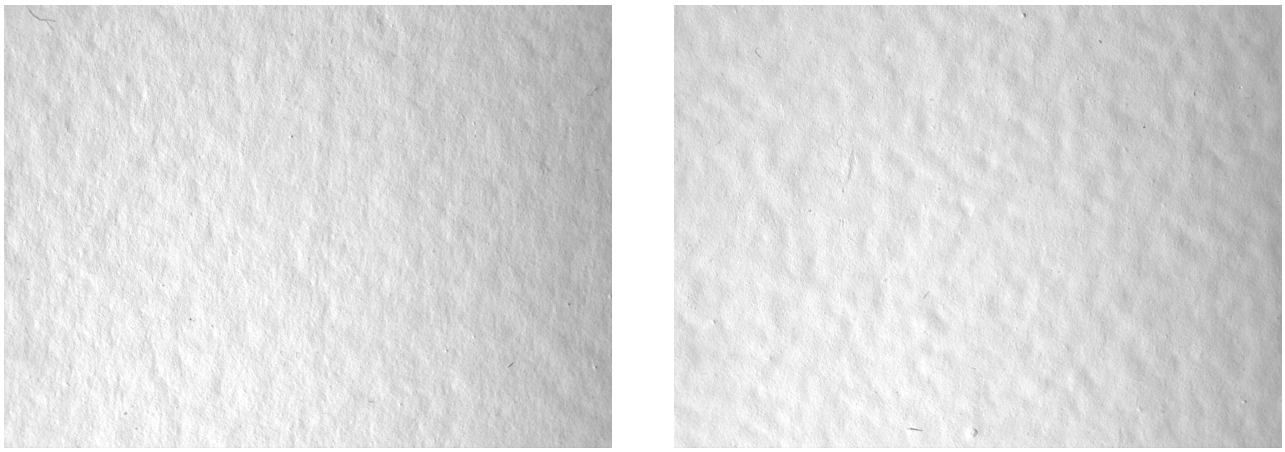

Figure 38: Images of Sample 2 obtained as a part of the photometric stereo method. The left image represents the rolled base coat and the right image shows the rolled touch-up coat.

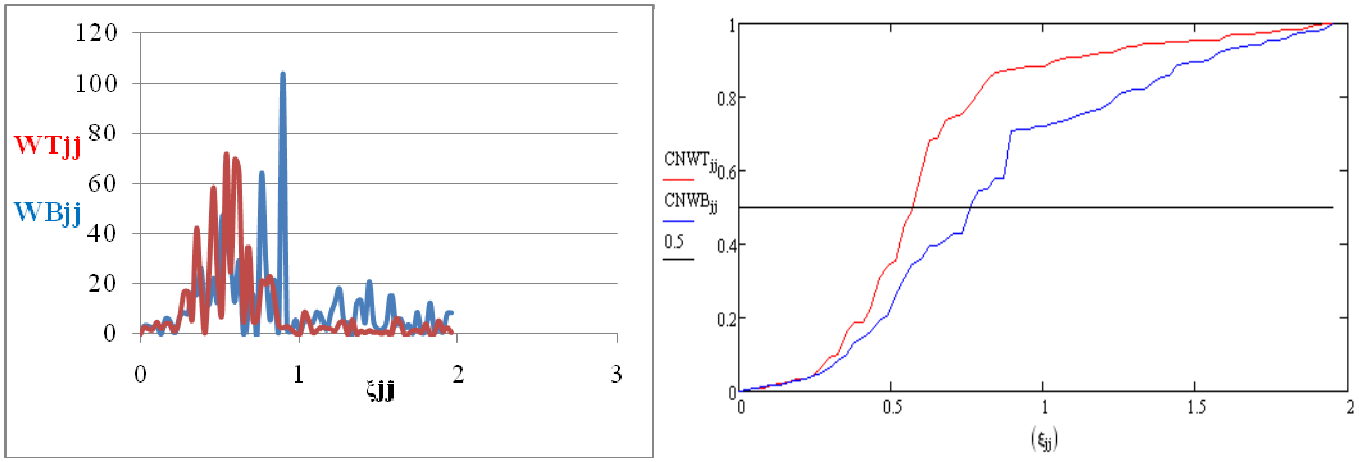

Figure 39: The graph on the left is of the noise power spectra of the base (WB, blue) and the touch-up (WT, red) regions. Note that the spectrum for the base and touch-up shows similar bandpass. The graph on the right is of the cumulative noise power spectra for the base and touch-up.

A comparison of the graphs for the two samples shows that a much greater variation can be seen between the base and the touch-up in the case of the sprayed sample than the rolled sample. This indicates that touching up a sprayed sample with a roller causes a much greater distinction between the textural properties of the two regions, thus making it a more detectable difference than touching up a rolled sample using a roller again. This is in accordance with what is observed with these two conditions.

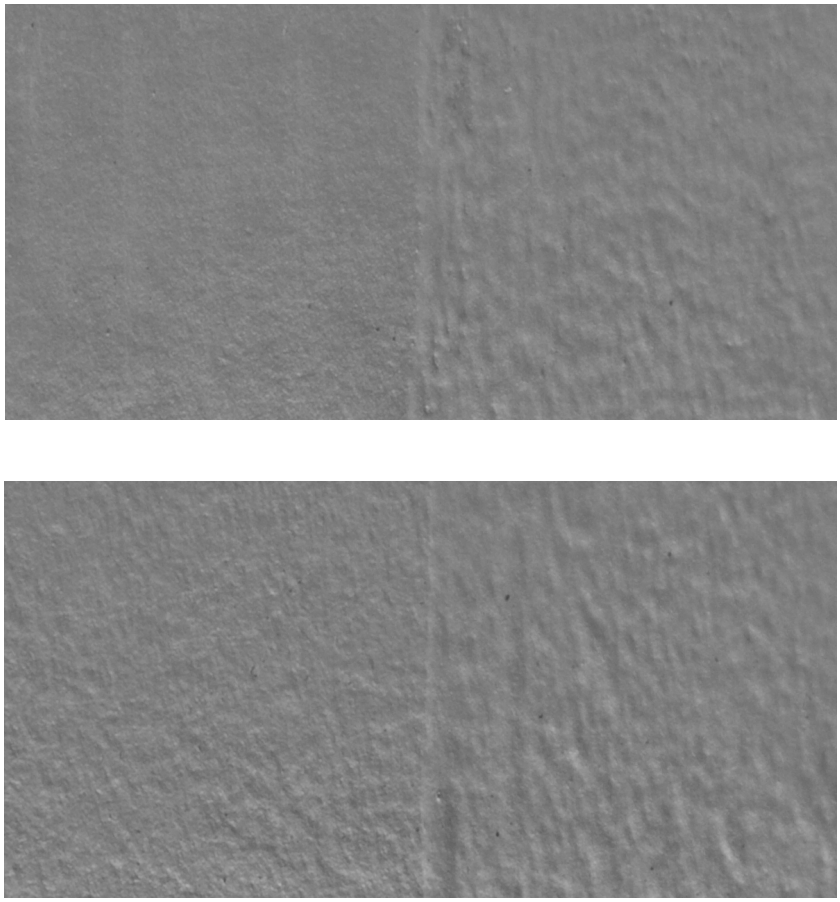

Figure 40: The upper image represents a region of Sample 1 with a sprayed base coat (left side) and rolled touch-up coat (right side). The texture differences between the two regions can be compared to those observed in Sample 2 (lower image) which has a rolled base and touch-up coat.

4.3 DISCUSSION

The following section consists of the consolidated results of the BRDF and surface measurements of each of the six samples. The top of the each page consists of the images obtained of the base and touch-up regions individually, using the photometric stereo method. The middle of the page consists of the BRDF data obtained from the Murakami gonio-spectrophotometer instrument. As described earlier, the open circles show the data obtained for the base region (left) and touch-up region (right) respectively. Finally the bottom of the page consists of the results from the noise power analysis of the frequency distribution of the normal angles. The graph on the left represents the noise power of the base and touch-up regions (WB_{jj} and WT_{jj} respectively) in terms of the spatial frequency of the elements in cycle/mm (ξ_{jj}). The graph on the left is the cumulative noise power spectra for the base and touch-up ($CNWB_{jj}$ and $CNWT_{jj}$ respectively) versus the frequency in cycles/mm (ξ_{jj}).

A discussion of the conclusions from these sets of results follows the data.

SAMPLE 1- AIRLESS SPRAYED BASE, PAINT A

Images of the base (left) and touch-up (right) region taken during experimentation

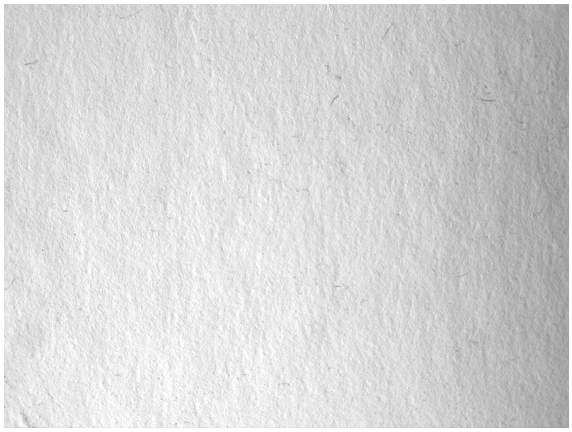

Graphs of the BRDF data

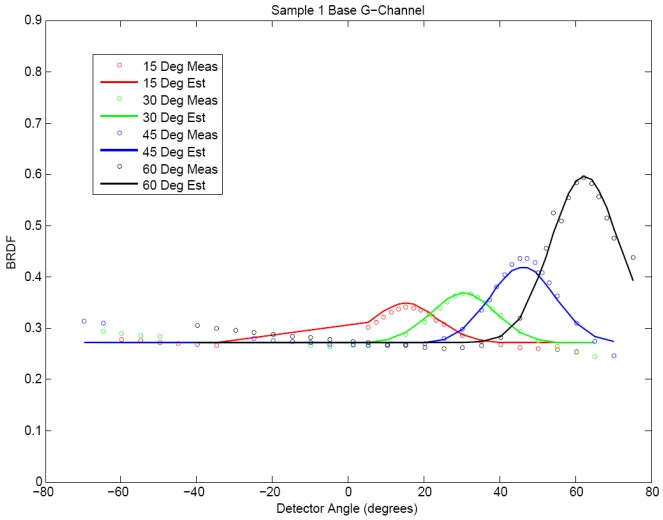

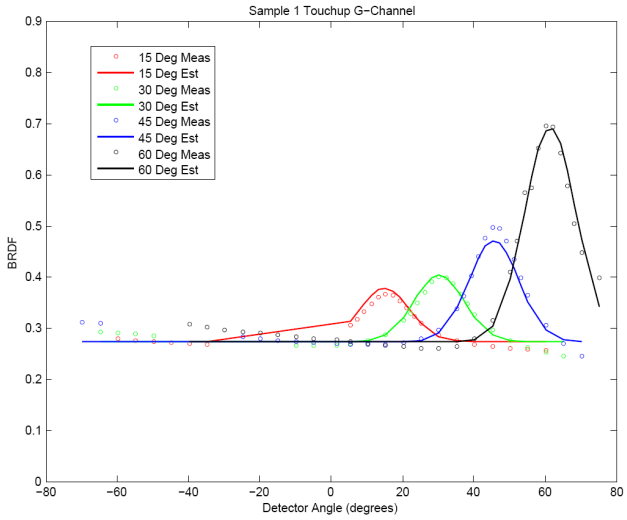

Graphs of the Noise Power analysis (left) and the Cumulative Noise Power Spectrum (right)

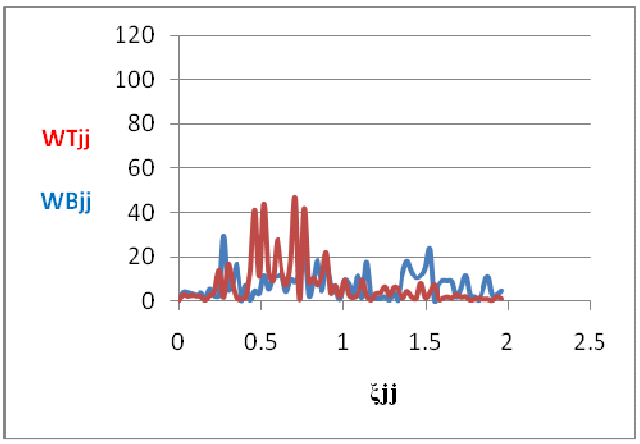

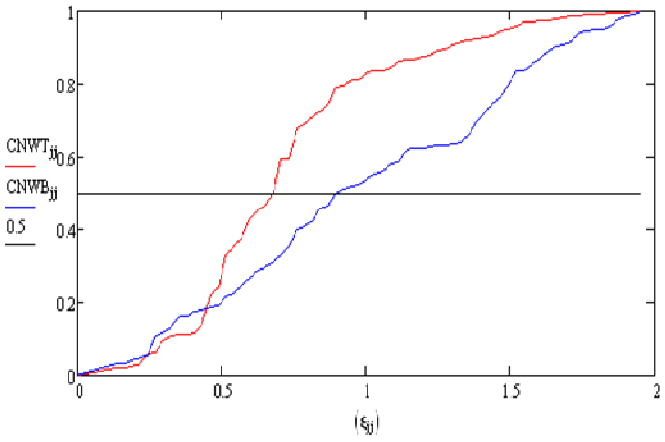

SAMPLE 2- ROLLED BASE, PAINT A

Images of the base (left) and touch-up (right) region taken during experimentation

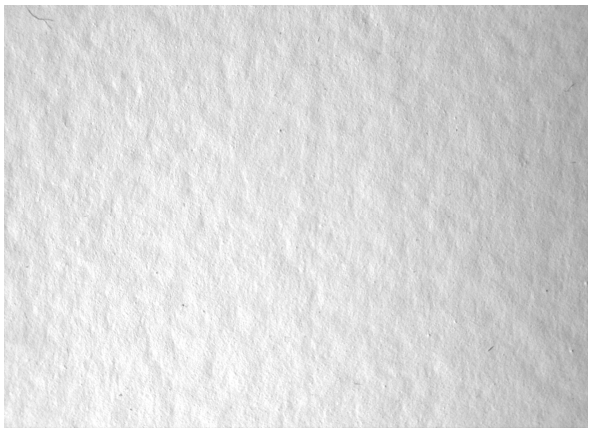

Graphs of the BRDF data

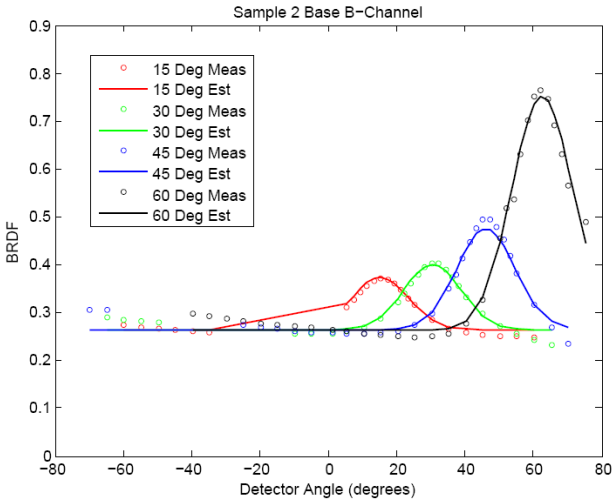

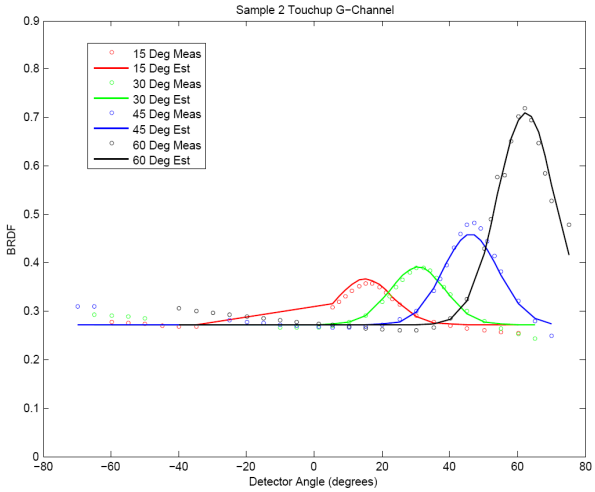

Graphs of the Noise Power analysis (left) and the Cumulative Noise Power Spectrum (right)

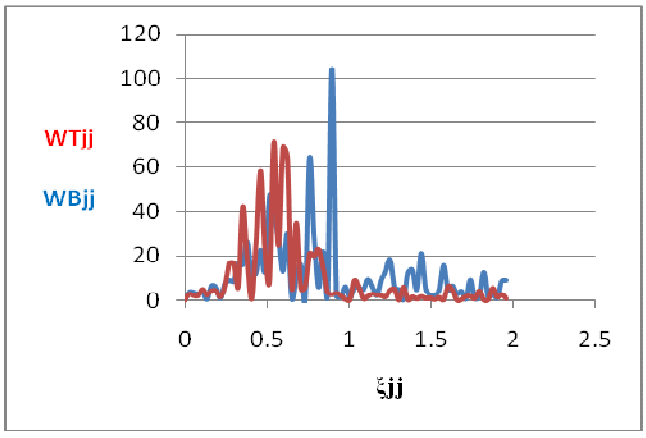

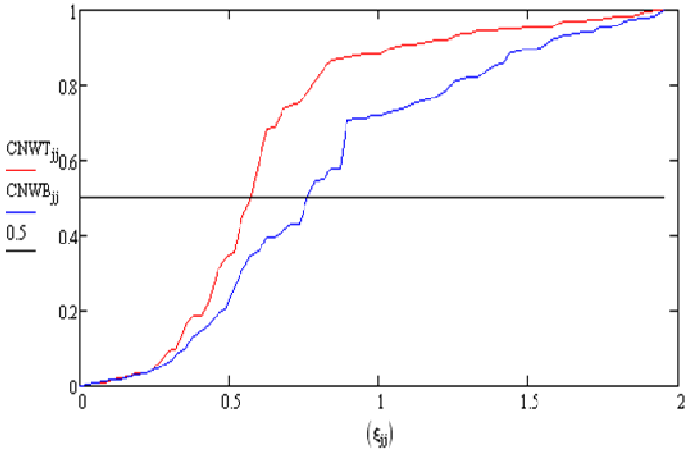

SAMPLE 3- AIRLESS SPRAYED BASE, PAINT B

Images of the base (left) and touch-up (right) region taken during experimentation

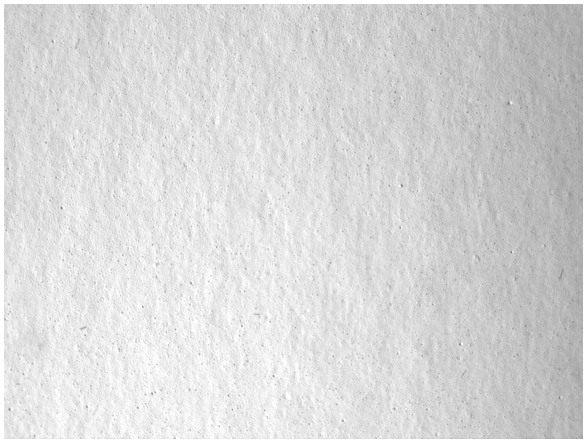

Graphs of the BRDF data

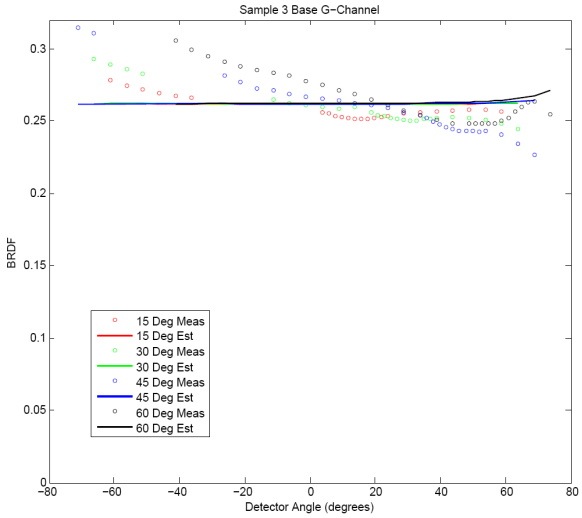

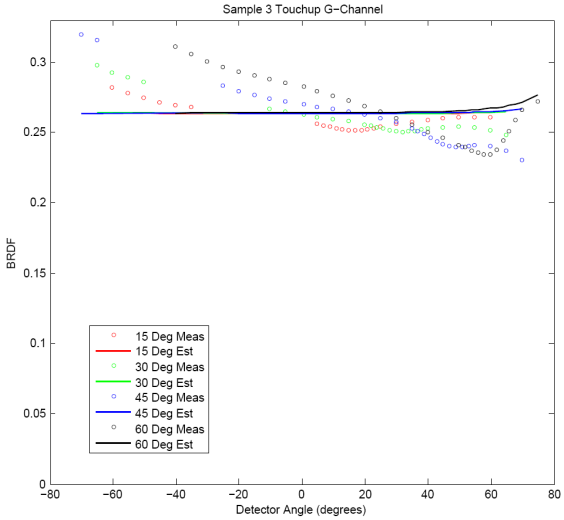

Graph of the Noise Power analysis (left) and the Cumulative Noise Power Spectrum (right)

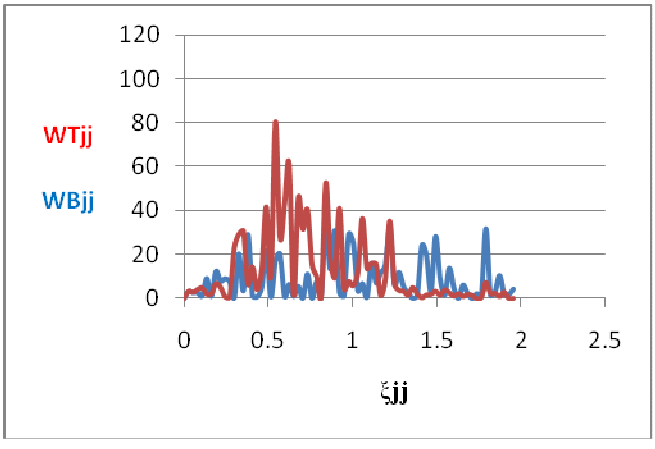

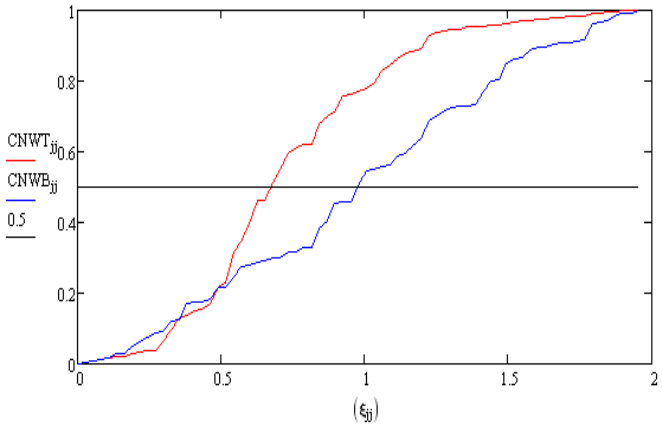

SAMPLE 4- ROLLED BASE, PAINT B

Images of the base (left) and touch-up (right) region taken during experimentation

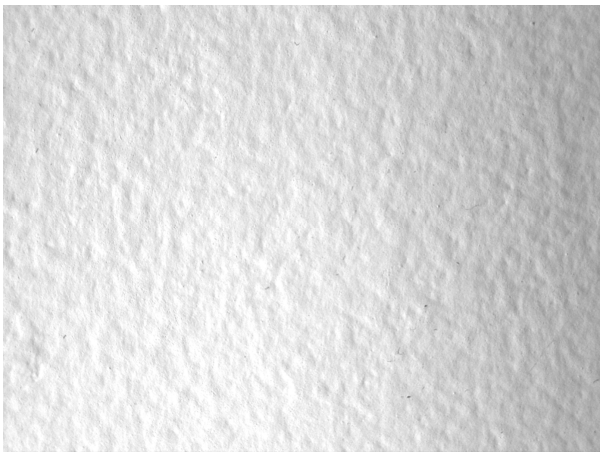

Graphs of the BRDF data

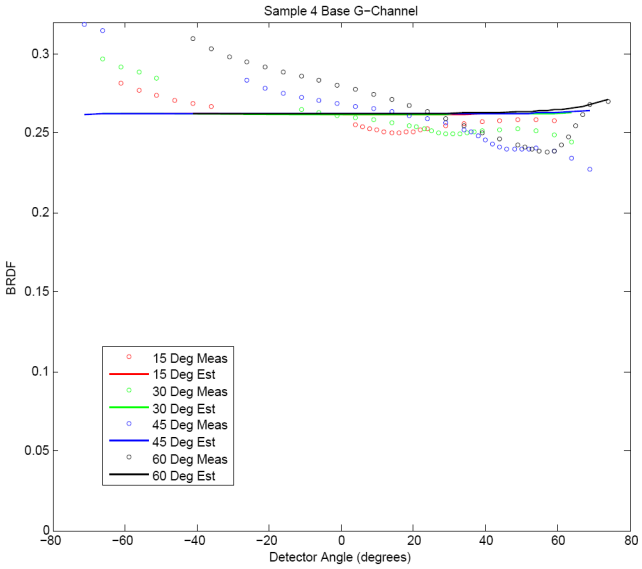

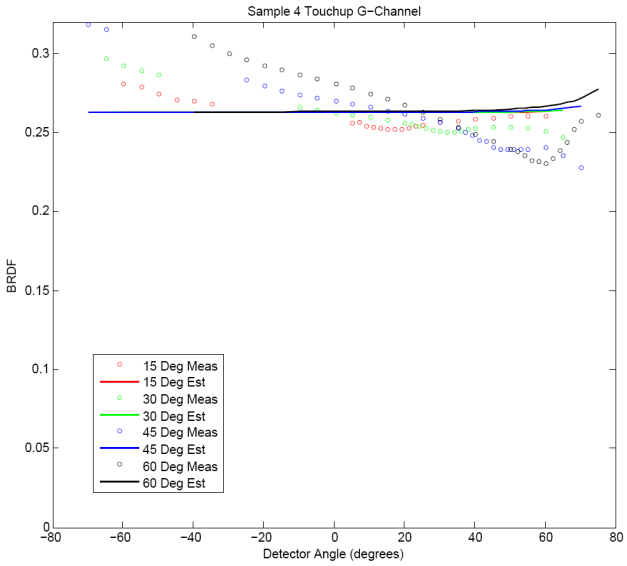

Graph of the Noise Power analysis (left) and the Cumulative Noise Power Spectrum (right)

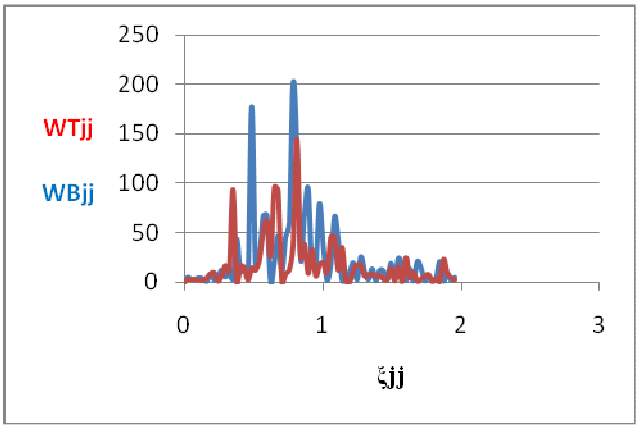

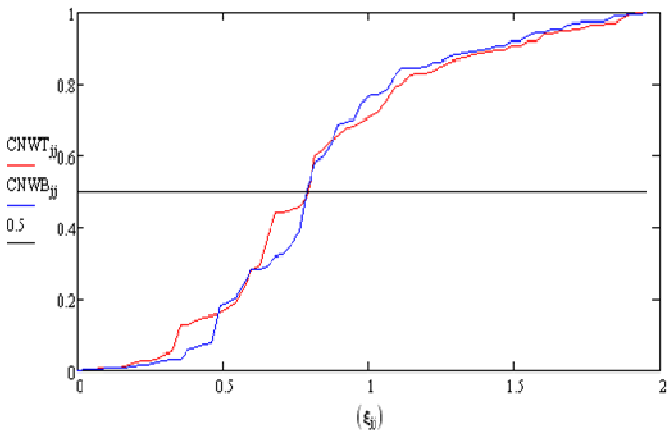

SAMPLE 5- AIRLESS SPRAYED BASE, PAINT C

Images of the base (left) and touch-up (right) region taken during experimentation

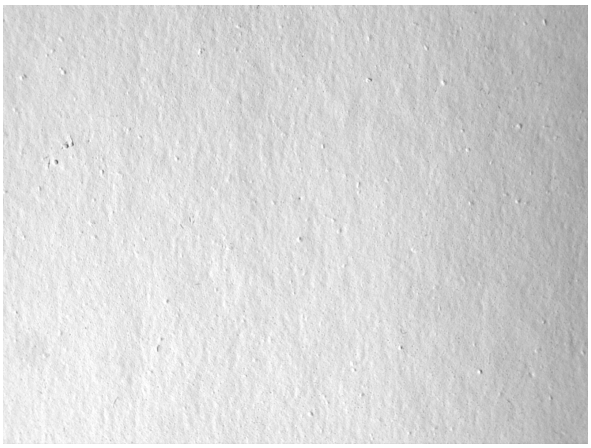

Graphs of the BRDF data

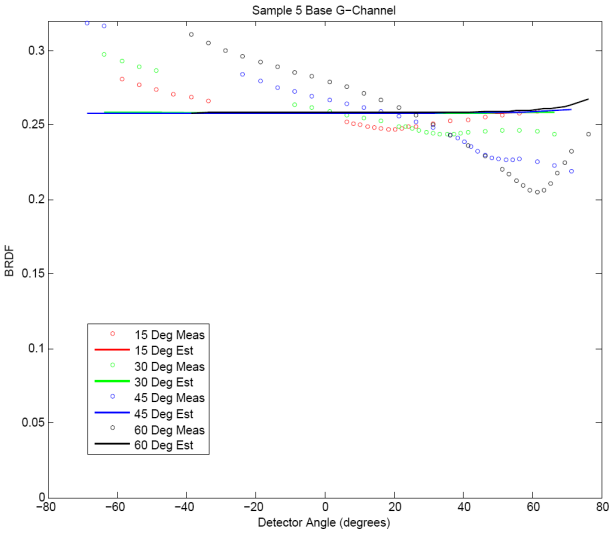

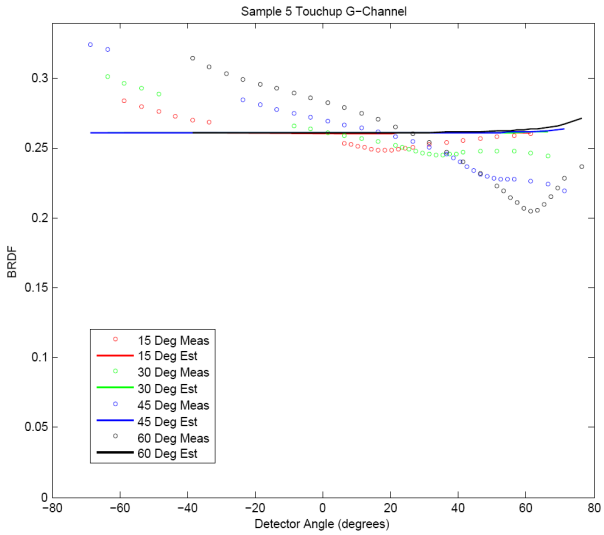

Graphs of the Noise Power analysis (left) and the Cumulative Noise Power Spectrum (right)

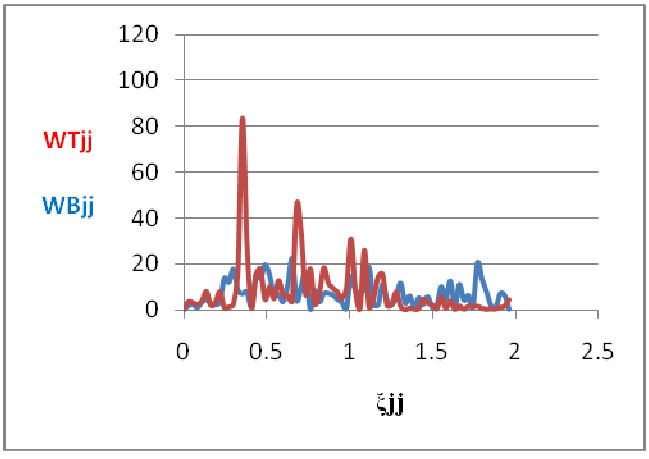

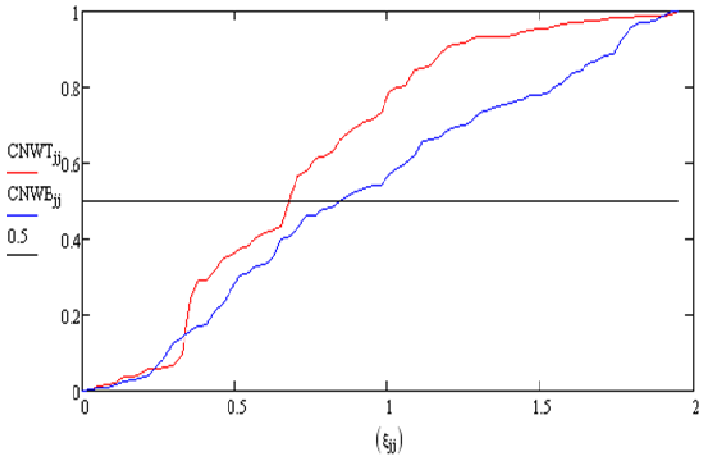

SAMPLE 6- ROLLED BASE, PAINT C

Images of the base (left) and touch-up (right) region taken during experimentation

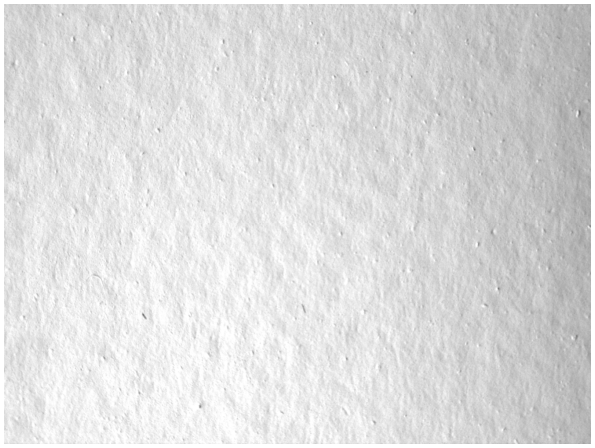

Graph of the BRDF data

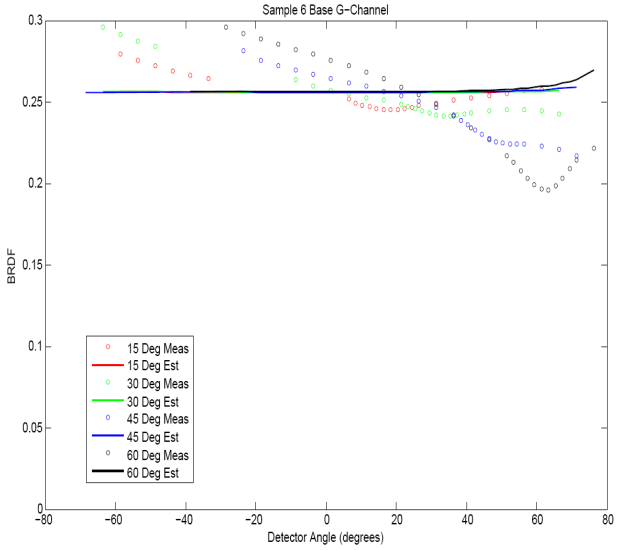

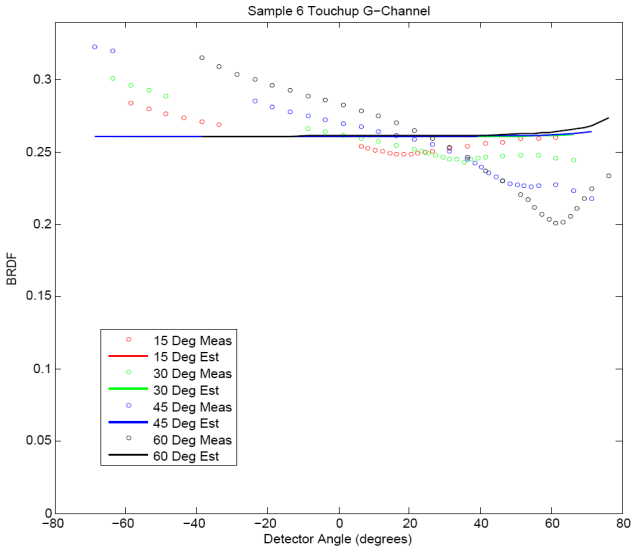

Graph of the Noise Power analysis (left) and Cumulative Noise Power Spectrum (right)

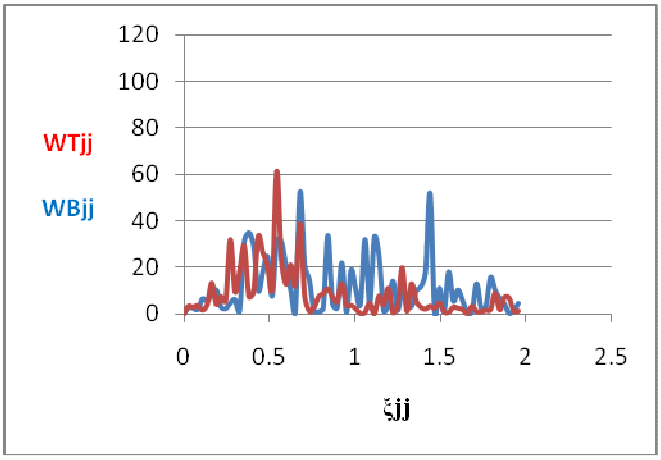

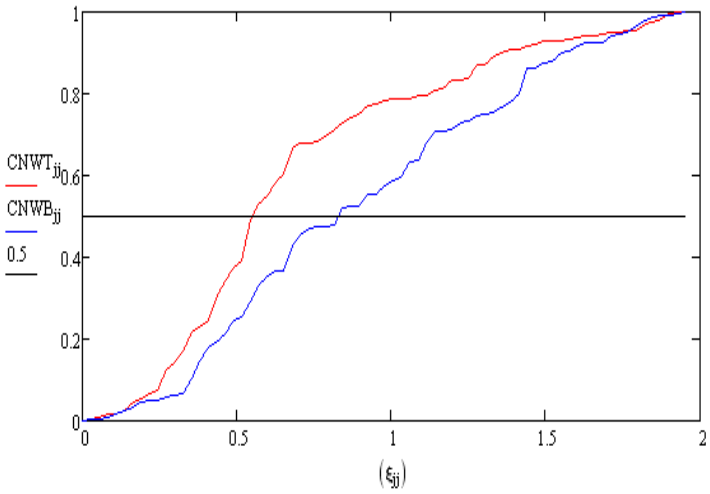

4.3.1 COMPARISON BETWEEN SPRAY AND BACKROLL APPLICATION METHODS

A comparison between the mesoscale texture of a sprayed base and rolled touch-up, versus a rolled base and rolled touch-up region has already been done in Section 3.2. To summarize this, in the common situation where a base coat is applied using airless spray and a region is touched-up over it using a roller, the base shows a broad-band behavior whereas the touch-up demonstrates a band-pass behavior. This means that *visually*, *the base is smoother than the touch-up*. At the microscale however, the higher and narrower distributions of the BRDF data indicate that the *touch-up region is optically smoother than the base*. This is the reason why the base region looks more matte and darker at grazing angles, whereas touch-up region looks glossy and lighter.

On the other hand, when the base and touch-up region are both rolled, the visual differences in texture are significantly reduced. The graphs of noise power show a similar band-pass behavior for both the base and touch-up regions. This clearly indicates the application method is a significant contributor to the magnitude of the touch-up problem

4.3.2 COMPARISON BETWEEN PAINTS A, B, AND C

An interesting behavior is seen in the BRDF measurements for the three kinds of paints. For samples on which Paints B and C are used, backscattering is found to be a predominant feature. Backscattering takes place when the light source and the detector are on the same side of the normal. In such a scenario, the sample radiates more energy back in the direction of the source than in the normal or forward direction. Backscattering intensity of paint depends on the scattering characteristics of the paint film and the amount of light transmitted into the film. This, in turn, is governed by the refractive index of the paint (Elton, 2008). Visual comparison of the painted samples indicate that Paint A is a glossier compared to paints B and C. This is the reason the lightness differences observed between the base and touch-up regions at grazing angles are more significant in Paint A. Hence, in addition to texture differences, another reason for touch-up visibility is lightness differences caused due to difference in gloss between paints.

5 SURFACE MODELING AND RENDERING

The measurement phase of the project focused on collecting data pertaining to the reflectance and surface texture properties of the samples. In order to correlate these physical properties with visual appearance, it is important to develop a model that will effectively describe the behavior of the touched-up surfaces. Therefore, in the modeling phase of the project, first, the reflectance data gathered in the measurement phase is modeled using a physically-based light reflection models such as Cook-Torrance, Ward etc. The parameters of this model serve as input data to a physically-based computer graphics rendering algorithm to create photometrically accurate and visually realistic synthetic images of objects. The parameters can also be varied systematically to develop a range of images representing different levels of touch-up visibility. The images thus obtained can be used as stimuli for a more controlled set of psychophysical experiments. The results of these experiments would help to determine the specific surface or paint formulation properties that control the visibility of the touch-up region.

5.1 SURFACE MODELING

Given a light source, a surface and an observer, a reflectance model describes the intensity and spectral composition of the reflected light reaching the observer. This is determined by the intensity of the light source and the reflecting ability and the surface properties of the material.

Using the BRDF data gathered in the measurement phase, the reflectance properties of the base and touch-up regions were modeled using the Cook-Torrance light reflection model. The Cook-Torrance model describes surface reflectance in terms of five terms- surface roughness, specular reflectance (ρ_s), diffuse reflectance (ρ_d), and real and imaginary refractive indices (η_{real}, $\eta_{imaginary}$). This model was used because of its effectiveness in handling nearly diffuse materials, such as the paint samples and its modeling of Fresnel effects (Cook & Torrance, 1981).

In order to fit the BRDF data effectively, we first convert the geometry of the Murakami

measurement system to the BRDF polar angle coordinates and then write a function that uses these four BRDF angles as parameters and returns an estimate of the BRDF value for the model one is fitting. A non-linear optimization is run to fit the BRDF model parameters to the dataset.

The graphs in Figures 41 and 42 demonstrate the fits obtained by the Cook-Torrance model to the measured BRDF data. In order to demonstrate the results, the graphs for samples 1 and 6, representing Paints A and C respectively, have been reproduced below. The open circles show the data obtained by measurement (as described in Section 4). The solid lines show the fits obtained to the BRDF data using the Cook-Torrance model. A good fit can be judged by how closely the estimates from the Cook-Torrance model match the BRDF data measured by the Murakami gonio-spectrophotometer.

Let us consider Figure 41 first, representing Sample 1- Paint A. As can be observed, overall, in the forward scattering direction (positive detector angles) the fits obtained are good. At negative detector angles, some backscattering effects were found. In this behavior, the surface radiates more energy in the direction of the source, than in the normal or forward direction.

If we compare this to the fits obtained for Sample 6, it is observed that backscattering was found to be a lot more significant in Paint C. No peak is observed at specular angle, which could be due to shadowing or masking effects from the larger scale texture. The sample appears to resemble a pure Lambertian surface (hence the straight line approximation by the Cook-Torrance model).

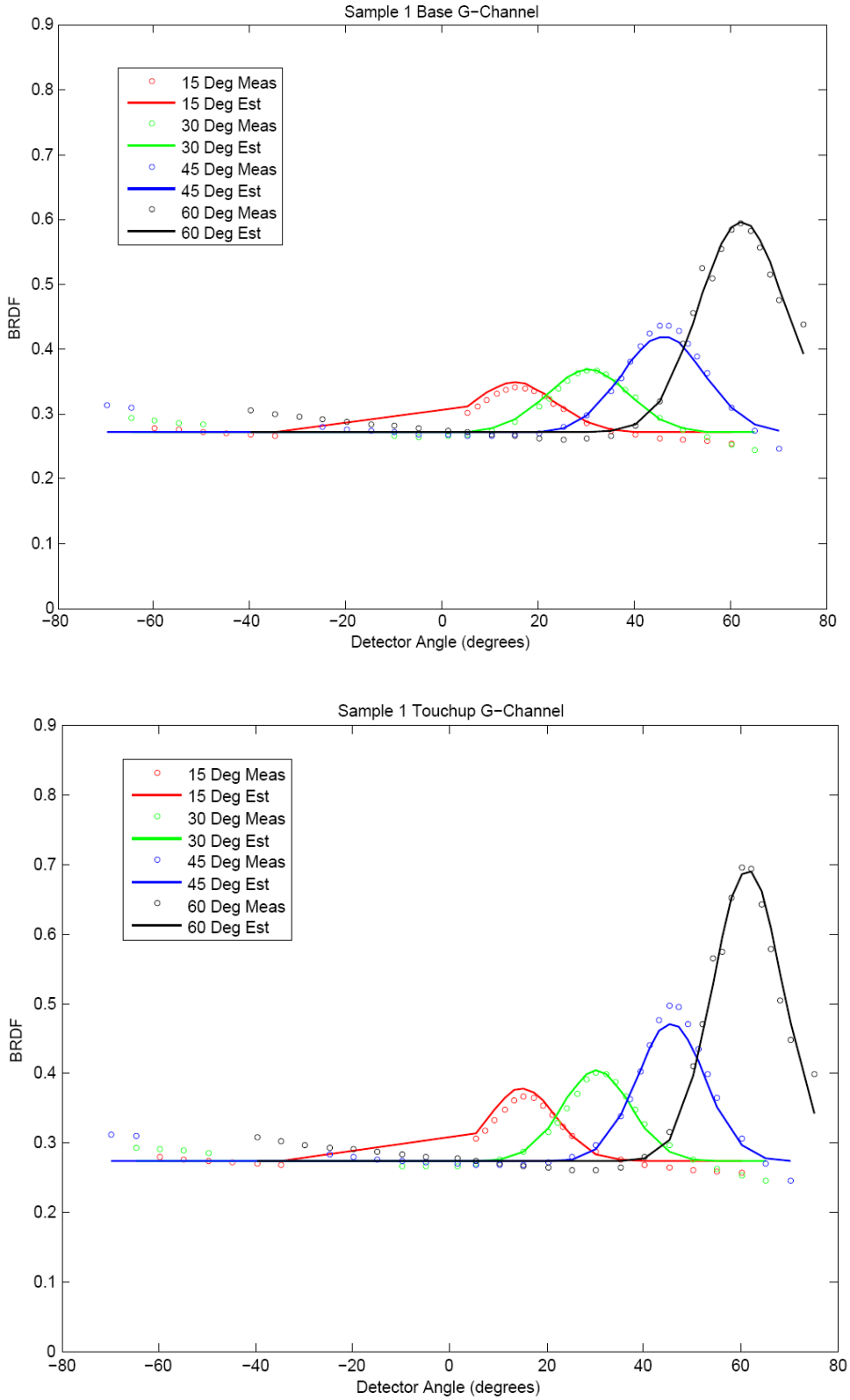

Figure 41: BRDF measurements for the sprayed base (top) and rolled touch-up regions (bottom)

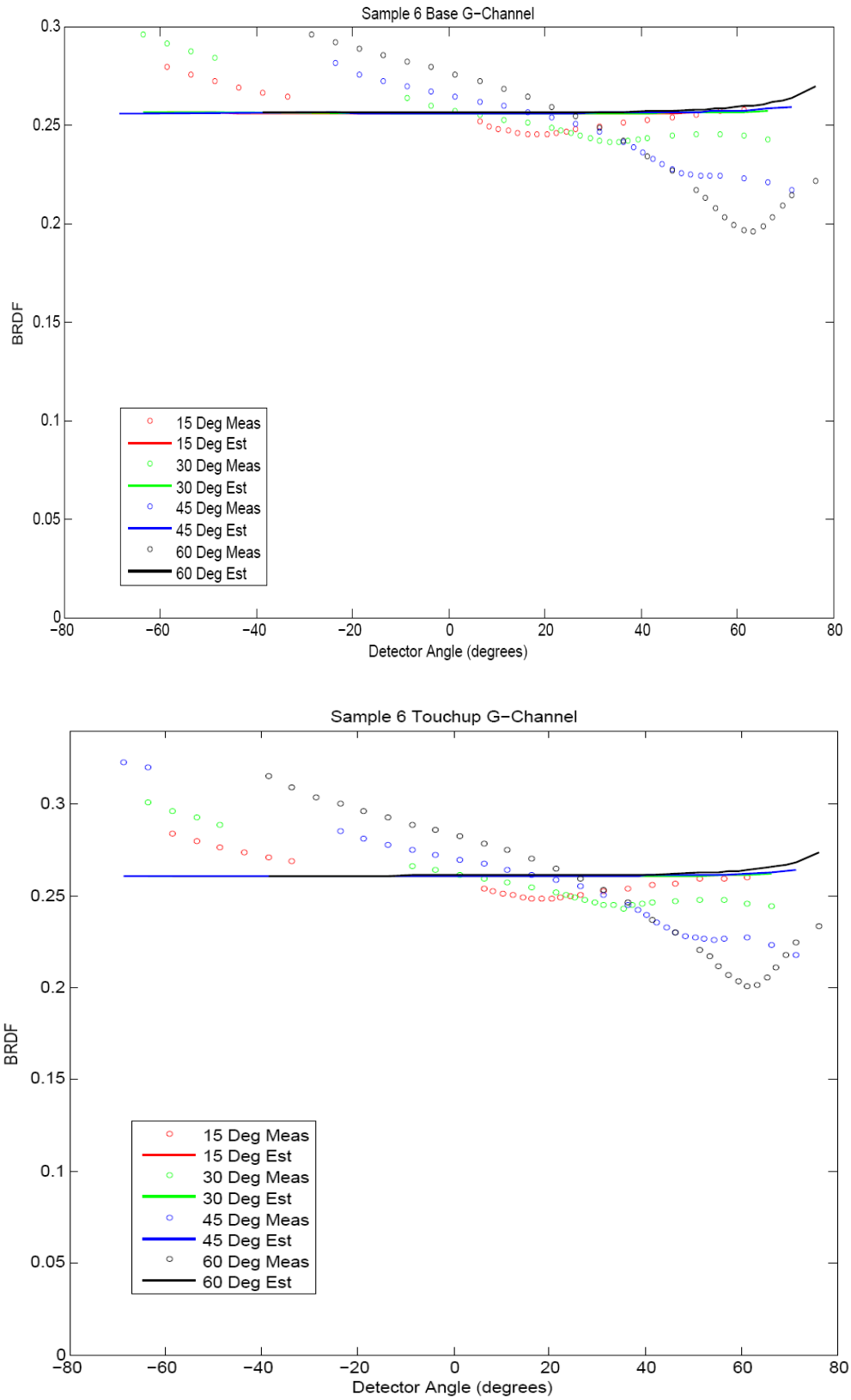

Figure 42: BRDF measurements for the rolled base (top) and rolled touch-up regions (bottom)

5.2 RENDERING

Physically-based computer graphics rendering techniques were used to create synthetic images of the painted samples. Geometric representations of the center-surround panels were created using the normal maps. Material properties were set using the Cook-Torrance fits to the BRDF data. The resulting models were illuminated with a simulated point light source placed 10 feet from the surface at an angle of 60 degrees to the surface normal. The rendering geometry is shown in Figure 43.

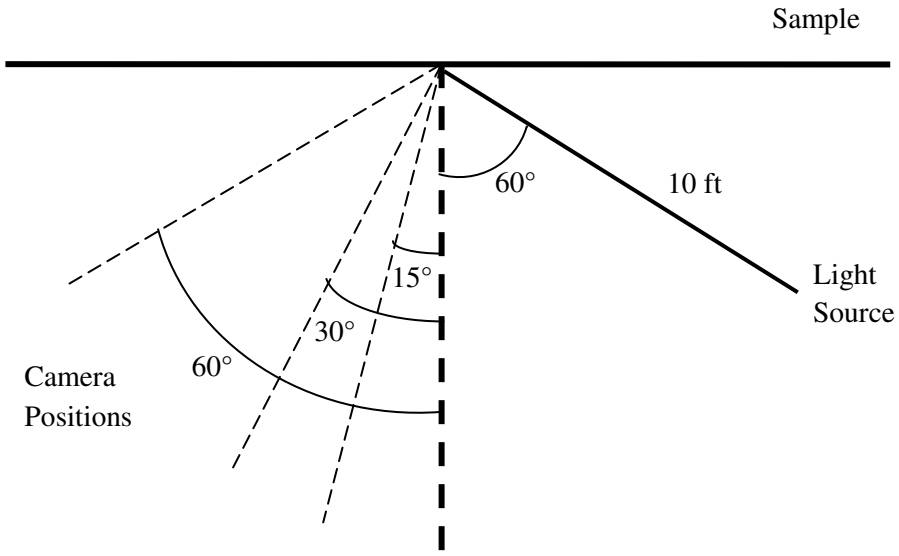

Figure 43: Rendering layout used to generate the synthetic images

The images in Figure 44 show the synthetic images of the samples generated by this process. These images are for Sample 1- with the spray base coat and rolled touch-up. From left to right, the images show the surface viewed at 0, 15 and 60 degrees with respect to the normal. At a standard 14 inch document viewing distance, the scale of features in the images is equivalent to viewing the sample from approximately 3 feet.

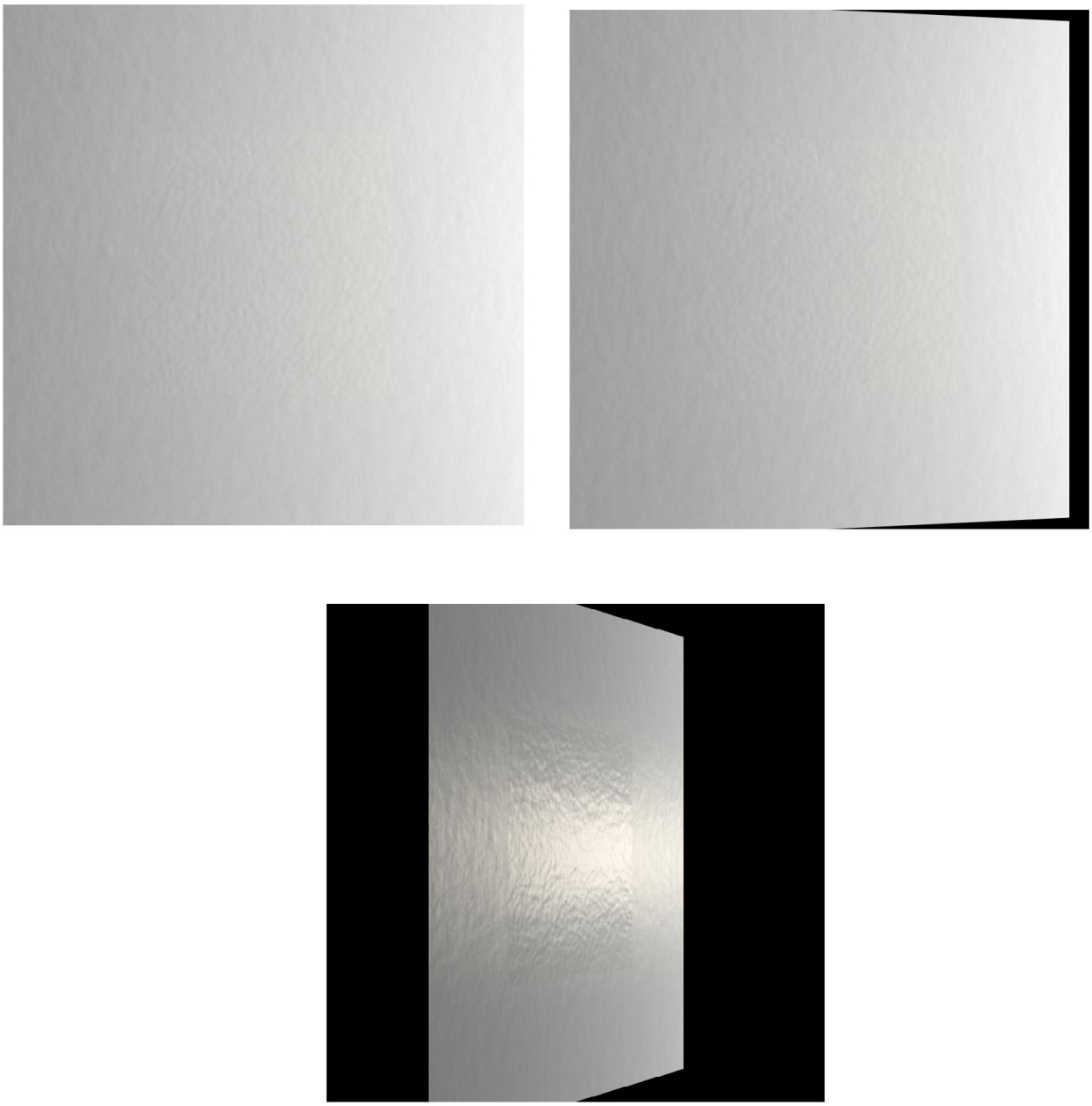

Figure 44: Renderings obtained with camera at 0° (top-left), 15° (top-right) and 60° (bottom)

These rendering do capture the touch-up phenomenon, since the differences between the base and touch-up are nearly indistinguishable at near-normal viewing angles, but start becoming more prominent at specular angles. However, the touch-up region looks glossier than the base when illuminated and viewed from oblique angles.

6 CONCLUSIONS

The “touch-up problem” is a very real problem being faced in the commercial paint industry. It decreases the aesthetic appearance of a painted surface, which in effect reduces customer satisfaction. Therefore, this research is an important first step in understanding the physical and perceptual aspects of the touch-up problem. The overall goal of the project is to derive quantitative information about the material parameters that need to be controlled in order to minimize the touch-up effect and to provide guidance on how to measure these parameters physically.

The samples used in this research were created by applying flat latex paint to standard wallboard surfaces. Two commonly used application methods- spraying and rolling were used. Initially, psychophysical experiments were conducted, using photographs of the painted samples as stimuli. Two experiments were conducted of which the first experiment aimed to determine the effect of paint formulation, application method, illumination and viewing conditions on the visibility of the touch-up region. The second experiment used a subset of the stimuli from the first experiment, in order to understand the effect of the type of edge on the touch-up visibility. A two-alternative forced choice design was used for the experiments and the judgments made by the subjects were used to create a Thurstonian scale to produce psychophysical scales of visibility. This scale provided valuable qualitative information regarding the factors that govern the touch-up effect. For example, it was found that while the overall appearance of a surface is governed by an interaction of various factors, the paint formulation and application methods were the most significant contributors. Also, a well-blended edge helped to reduce touch-up differences greatly, compared to an irregular rough edge. We were also able to compare the behavior of different types of paints in enhancing or reducing this effect.

The next step was to relate the visual appearance to surface properties. Visual inspection of the painted surfaces showed that the base and touch-up regions differ in terms of their reflectance properties and their texture. The reflectance properties of a surface are characterized by their Bi-directional Reflectance Distribution Function (BRDF). The Murakami gonio-spectrophotometer was used to measure the BRDF of the base and touch-up regions of each sample individually. It was found that the touch-up region is optically smoother than the base region, which causes it to

appear lighter than the base at grazing angles. Also, a glossier paint shows greater differences at grazing angles than a matte paint. To measure texture properties of the surfaces, the photometric stereo method was used. A noise power analysis of the data showed that a rolled touch-up region has more energy over a band of lower frequencies, whereas a sprayed base has an even distribution of energy over a wide range of frequencies. This means that the base is visually rougher than the touch-up region, causing textural differences. If these results are combined, we can conclude that the touch-up effect is due to the interaction of the lightness and texture differences, each operating at a different scale. Hence, in the initial stages of the research, we were able to successfully capture the surface reflectance and texture properties.

These measurement data were then fit to the Cook-Torrance light reflection model. Back-scattering was found to be a significant factor in some of the paint formulations, which was not captured effectively by this model. The parameters of the Cook-Torrance model were then used as input for a physically based image synthesis algorithm to generate realistic images of the paint surfaces. Figure 46 is a reproduction of the initial set of renderings that were obtained. While an initial workflow has been established, there is still scope for further development in this domain. The challenges faced at this stage and the next steps in this research have been described in the next section.

6.1 LIMITATIONS AND FUTURE WORK

Any surface has structure across a continuum of scales. In order to understand the critical spatial scales that affect the touch-up problem, it is important to understand the contribution of the microscale (reflectance) and mesoscale (texture) *independently* to the surface appearance. Consider the renderings in Figure 45 which have been developed using the same rendering algorithm described in Section 4.2. These are shader views (on-axis views for an off-axis camera angle) of Sample 1. The left image represents the shader view for the camera angle at 15° whereas the right image represents the shader view for a camera angle of 60°. If we compare these renderings with the actual photograph of the same sample taken at an off-axis camera angle of 60° (Figure 46), we can see that there is a gap in the actual versus synthetic reproduction of the same surface.

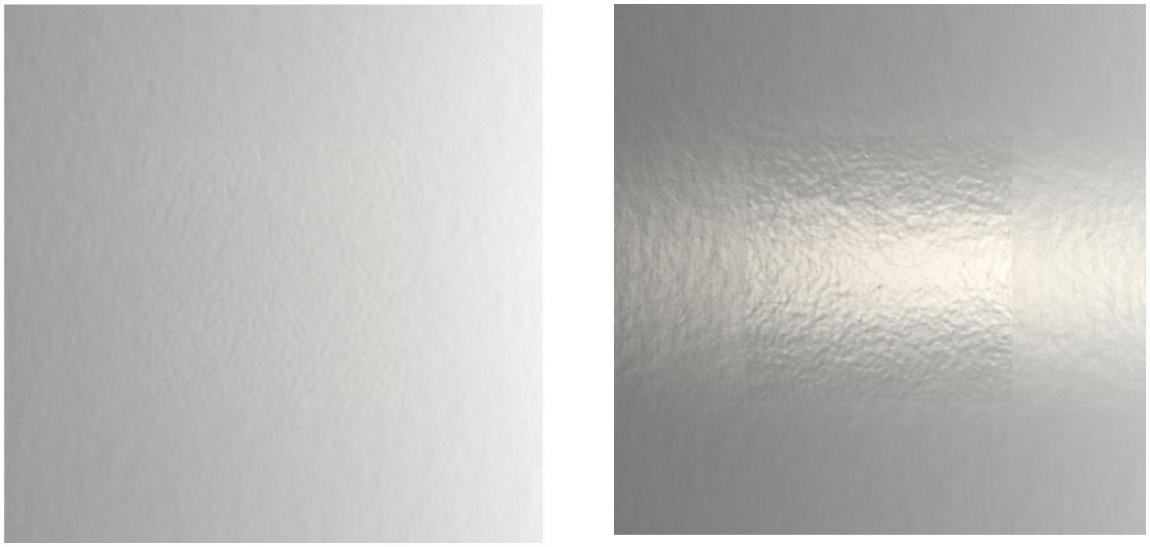

Figure 45: On-axis views of renderings for off-axis camera angles of 15° (left) and 60° (right)

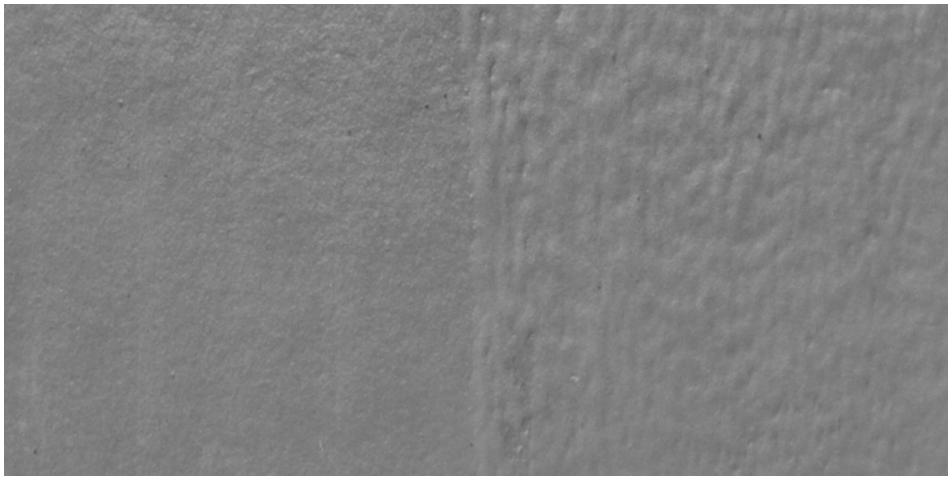

Figure 46: Image of sample captured at a camera angle of 60°

We have identified what is called the “double-counting problem” from these simulations. Most conventional instruments would show an overlap of ranges over which measurements are made. In this particular case, due to its large acceptance angle, the sensor in the gonio-spectrophotometer is incorporating the effects of mesoscale texture variations into its BRDF estimates (Wyble & Berns, 2010). If these BRDF measurements are used along with

the texture geometry measurements to render computer graphics images, the mesoscale texture is included twice in the calculations. This is causing inaccuracies in the rendered images. The solution is to use one instrument to measure both the BRDF and surface texture. This can be done using a form of an imaging gonio-reflectometer constructed using a digital camera, a light source and a protractor arm to mount the sample. The images captured using this setup can be used to simultaneously extract surface normal maps and point-wise estimates of the BRDF that are not contaminated by the "double counting problem".

The data captured using this instrument can be varied parametrically to explore the effects of reflectance and texture on touch-up visibility. Given the backscattering phenomenon observed in paints B and C, there might be a necessity to fit the BRDF data to a reflectance model developed from first principles. The design of parametric texture models is an emerging research area, but there are various parameterizations such as Fourier, fractal, wavelet etc. which can be investigated. These reflectance and texture parameters can be systematically varied in computer graphics simulations, which would in turn serve as stimuli for a series of perceptual experiments. These experiments would help to provide more in-depth information on the relationships between surface reflectance, geometry, illumination, and viewing conditions and the visual qualities and magnitudes of the touch-up problem. The eventual goal is to develop a psychophysical model of the touch-up problem that relates the physical differences in paint formulation and application methods to visual differences in surface appearance. This model can then be used to allow paint manufacturers, architects, designers and contractors to understand how and why the touch-up problem occurs, and to determine how to adjust formulations and/or application methods to minimize the problem.

7 REFERENCES

1. Arney, J. S., Jiff, W., Oswald, T., & Ye, L. (2006). Analysis of Paper Gloss. *Journal of Pulp and Paper Science, 32*.
2. Arney, J. S., & Nilosek, D. R. (2007). Analysis of Print Gloss with a Calibrated Micro-Goniophotometer. *The Journal of Imaging Science and Technology, 51*, 509-513.
3. Arney, J. S., Peter, A., & Hoon, H. (2004). A Micro-Goniophotometer and the Measurement of Print Gloss. *Journal of Imaging Science & Technology, 48*.
4. Arney, J. S., & Stewart, D. (1993). Surface Topography of Paper from Image Analysis of Reflectance Images. *Journal of Imaging Science & Technology, 37*.
5. Arney, J. S., Tantalo, T., & Stewart, D. (1994). The Measurement of Surface Topography of Materials by Analysis of Goniometric Reflection of Light: Factors Governing Precision and Accuracy. *Journal of Imaging Science & Technology, 38*.
6. Arney, J. S., Ye, L., & Banach, S. (2006). Interpretation of Gloss Meter Measurements. *Journal of Imaging Science & Technology, 50*.
7. AvianGroupUSA. (2009). Avian GroupUSA - Gonio - GCMS 3B. from http://www.aviangroupusa.com/murakami/gonio/gcms-3b.php
8. Blinn, J. F. (1977). *Models of Light Reflection for Computer Synthesized Pictures.* Paper presented at the SIGGRAPH.
9. Chen, Y. (2008). *Model Evaluation and Measurement Optimization for the Reproduction of Artist Paint Surfaces through Computer Graphics Renderings.* Rochester Institute of Technology, Rochester.
10. Cook, R. L., & Torrance, K. E. (1981). *A reflectance model for computer graphics.* Paper presented at the SIGGRAPH '81, Dallas, Texas.
11. Cornsweet, T. (1970). Visual Perception: Academic Press.
12. Elton, N. J., Legrix, A. (2008). Reflectometry of Drying Paint: Surfoptic Ltd.
13. Engeldrum, P. (2000). *Psychometric Scaling- A Toolkit for Imaging Systems Development*: Imcotek Press.

14. Ferwerda, J. A., Pellacini, F. and Greenberg.D.P. (2001). *A psychophysically-based model of surface gloss perception.* Paper presented at the Proceedings SPIE Human Vision and Electronic Imaging '01. Retrieved from http://www.cis.rit.edu/jaf/
15. Gescheider, G. A. (1997). *Psychophysics- The Fundamentals* (3rd edition ed.). Mahwah, NJ: Lawrence Erlbaum Associates.
16. Goral, C., Torrance, K. E., Greenberg, D. P., & Battaile, B. (1984). Modeling the interaction of light between diffuse surfaces. *Computer Graphics, 18*(3).
17. Greenberg, D. P., Torrance, K.T., Shirley, P., Arvo, J., Ferwerda, J.A., Pattnaik, S., Lafortune, E., Walter, B., S.Foo, B., Trumbore, A. (1997). *A Framework for Realistic Image Synthesis.* Paper presented at the SIGGRAPH.
18. Guilford, S. C. (1954). *Psychometric Methods* (2nd edition ed.): McGraw-Hill Book Company, Inc.
19. House-Painting-Info.com. (2009). Airless Paint Sprayers.
20. Hunter, R. S., & Harold, R. W. (1987). *The measurement of appearance* (2nd ed.). New York: Wiley.
21. Judd, D. B. (1937). Gloss and Glossiness: Am. Dyest.
22. Lafortune, E. P. F., Foo, S.-C., Torrance, K. E., & Greenberg, D. P. (1997). *Non-linear approximation of reflectance functions.* Paper presented at the SIGGRAPH '97: Proceedings of the 24th annual conference on Computer graphics and interactive techniques, New York.
23. Macey, J. (1997). *Ray-tracing and other Rendering Approaches- Lecture Notes*: University of Bournemouth.
24. Nicodemus, F. E., Richmond, J. C., Hsia, J. J., & Ginsberg, I. W. (1977). *Geometrical Considerations and Nomenclature for Reflectance*.
25. Nikodym, T. (2010). *Ray Tracing Algorithm for Interactive Applications.* Czech Technical University.
26. O'Donnel, F. (1984). *Psychometric Scaling of Gloss.* Rensselaer Polytechnic Institute.
27. O'Donnel, F., & Billmeyer, F. J. (1986). Psychometric Scaling of Gloss.
28. Oren, M., & Nayar, S., K. (1995). Generalization of the Lambertian model and implications for machine vision. *International Journal of Computer Vision, 14*.
29. Phong, B. T. (1975). Illumination for computer generated pictures. *Commun. ACM, 18*.

30. Thurstone, L. L. (1927). The method of paired comparisons for social values. *Journal of Abnormal and Social Psychology, 21*, 384-400.
31. Torrance, K. E., & Sparrow, E. M. (1967). Theory for Off-Specular Reflection from Roughened Surfaces. *Journal of the Optical Society of America, 57*.
32. Walter, B. (2005). *Notes on the Ward BRDF* (No. Technical Report PCG-05-06).
33. Ward, G. J. (1992). *Measuring and modeling anisotropic reflection*. Paper presented at the Proceedings of the 19th annual conference on Computer Graphics and Interactive Techniques. Retrieved from http://portal.acm.org/citation.cfm?id=133994.134078
34. Wiley, C., Romney, G. W., Evans, D. C., & Erdahl, A. (1967). *Halftone perspective drawings by computer*. Paper presented at the AFIPS FJCC.
35. Woodham, R. (1980). Photometric method for determining surface orientation from multiple images. *Optical Engineering, 19*.
36. Wyble, D. R., & Berns, R. S. (2010). *Validating the Accuracy of the MCSL Imaging Goniospectrometer*: Rochester Institute of Technology.